The Company of **Biologists**

RESEARCH ARTICLE

PCMD-1 bridges the centrioles and the pericentriolar material scaffold in *C. elegans*

Lisa Stenzel[1], Alina Schreiner[1], Elisa Zuccoli[1], Sim Üstüner[1], Judith Mehler[1], Esther Zanin[1,2] and Tamara Mikeladze-Dvali[1,*]

ABSTRACT

Correct cell division relies on the formation of a bipolar spindle. In animal cells, microtubule nucleation at the spindle poles is facilitated by the pericentriolar material (PCM), which assembles around a pair of centrioles. Although centrioles are essential for PCM assembly, the proteins that anchor the PCM to the centrioles are less known. Here, we investigate the molecular function of PCMD-1 in bridging the PCM and the centrioles in *Caenorhabditis elegans*. We demonstrate that the centrosomal recruitment of PCMD-1 is dependent on the outer centriolar protein SAS-7. The most C-terminal part of PCMD-1 is sufficient to target it to the centrosome, and the coiled-coil domain promotes its accumulation by facilitating self-interaction. We reveal that PCMD-1 interacts with the PCM scaffold protein SPD-5, the mitotic kinase PLK-1 and the centriolar protein SAS-4. Using an ectopic translocation assay, we show that PCMD-1 can selectively recruit downstream PCM scaffold components to an ectopic location in the cell, indicating that PCMD-1 is able to anchor the PCM scaffold proteins at the centrioles. Our work suggests that PCMD-1 is an essential functional bridge between the centrioles and the PCM.

KEY WORDS: PCM, PCMD-1, PLK-1, SPD-5, Centrioles, Centrosome

INTRODUCTION

Centrosomes are dynamic, non-membranous organelles that serve as the major microtubule-organizing centers in animal cells and are thus essential for biological processes ranging from polarity establishment to the orchestration of cell division. Centrosomes comprise a centriole pair and the surrounding pericentriolar material (PCM). The size and material properties of the PCM change dynamically during the cell cycle (Woodruff et al., 2015, 2017; Mittasch et al., 2020).

PCM expansion during mitosis facilitates bipolar spindle assembly. At the root of PCM expansion is a proteinaceous matrix that serves as a scaffold for the recruitment of regulatory proteins, including mitotic kinases and microtubule nucleators. In *Caenorhabditis elegans*, this scaffolding function is fulfilled by self-assembly of the coiled-coil protein SPD-5 (functional homolog of human CDK5RAP2), which is controlled by phosphorylation through Polo-like kinase PLK-1 (homolog of human PLK1) and interaction with the coiled-coil protein SPD-2 (homolog of human

CEP192) (Hamill et al., 2002; Decker et al., 2011; Woodruff et al., 2015, 2017; Cabral et al., 2019). Our previous findings have revealed that PCMD-1, a protein with a predicted coiled-coil domain, regulates the spatial integrity of the PCM scaffold, and, together with SPD-2, is required for the recruitment of SPD-5 (Erpf et al., 2019). Centrioles serve as condensation centers for PCM proteins. During PCM expansion in mitosis, centrioles contribute to the growth and structural integrity of the PCM scaffold (Cabral et al., 2019). A limited set of centriolar core proteins has been described in *C. elegans* (O'Connell et al., 2001; Kirkham et al., 2003; Leidel and Gönczy, 2003; Dammermann et al., 2004; Delattre et al., 2004, 2006; Kemp et al., 2004; Pelletier et al., 2004, 2006; Leidel et al., 2005; Dammermann et al., 2008; Sugioka et al., 2017). From these proteins, SPD-2, SAS-4 (CPAP homolog) and SAS-7 have been proposed to functionally bridge the PCM and the centrioles (Varadarajan and Rusan, 2018). SAS-4, which localizes to the centrioles and the PCM, plays a crucial role in microtubule assembly around the central tube of a forming centriole (Kirkham et al., 2003; Leidel and Gönczy, 2003; Dammermann et al., 2008; Delattre et al., 2006; Pelletier et al., 2006). SAS-7 facilitates the formation of the paddlewheel structure on centriolar microtubules and recruits SPD-2, which in turn is needed for centriole duplication and mitotic PCM scaffold expansion (Sugioka et al., 2017).

PCMD-1 is predominantly a centriolar protein, yet its depletion affects SPD-5 recruitment and the structural integrity of the PCM (Erpf et al., 2019), raising the possibility that it connects the PCM scaffold functionally to the centrioles. However, the precise mechanisms of PCMD-1 centriolar targeting and how PCMD-1 recruits PCM components is still to be elucidated. Here, we investigate the function of PCMD-1 in functionally bridging centrioles and the PCM in *C. elegans* embryos.

RESULTS

SAS-7 maintains PCMD-1 at the centrioles in early embryos

PCMD-1 localizes weakly to the PCM and strongly to centrioles. PCMD-1 does not require the PCM scaffold protein SPD-5 for its localization in one-cell embryos (Erpf et al., 2019). This raises the questions of whether PCMD-1 is recruited to the centrosome via outer centriolar proteins and whether PCMD-1, in turn, has a role in maintaining these proteins at centrioles. One candidate for such interaction is SAS-7, which is needed for the formation of paddlewheels, the outermost centriolar structures known in *C. elegans* (Sugioka et al., 2017). We investigated the spatial relationship between PCMD-1 and SAS-7 by analyzing embryos expressing endogenously tagged GFP::PCMD-1 and RFP::SAS-7 using lattice structured illumination microscopy (SIM) (Fig. 1A). We found that PCMD-1 and SAS-7 signals largely overlapped on both centrioles at spindle poles of mitotic blastomeres in early embryos (Fig. 1A). This observation prompted us to test whether SAS-7 and PCMD-1 localization are interdependent. Live-cell

[1]Department Biology II, Ludwig-Maximilians-University, Munich, 82152 Planegg-Martinsried, Germany. [2]Department Biologie, Friedrich-Alexander-Universität Erlangen-Nürnberg, 91058 Erlangen, Germany.

*Author for correspondence (tmdvali@bio.lmu.de)

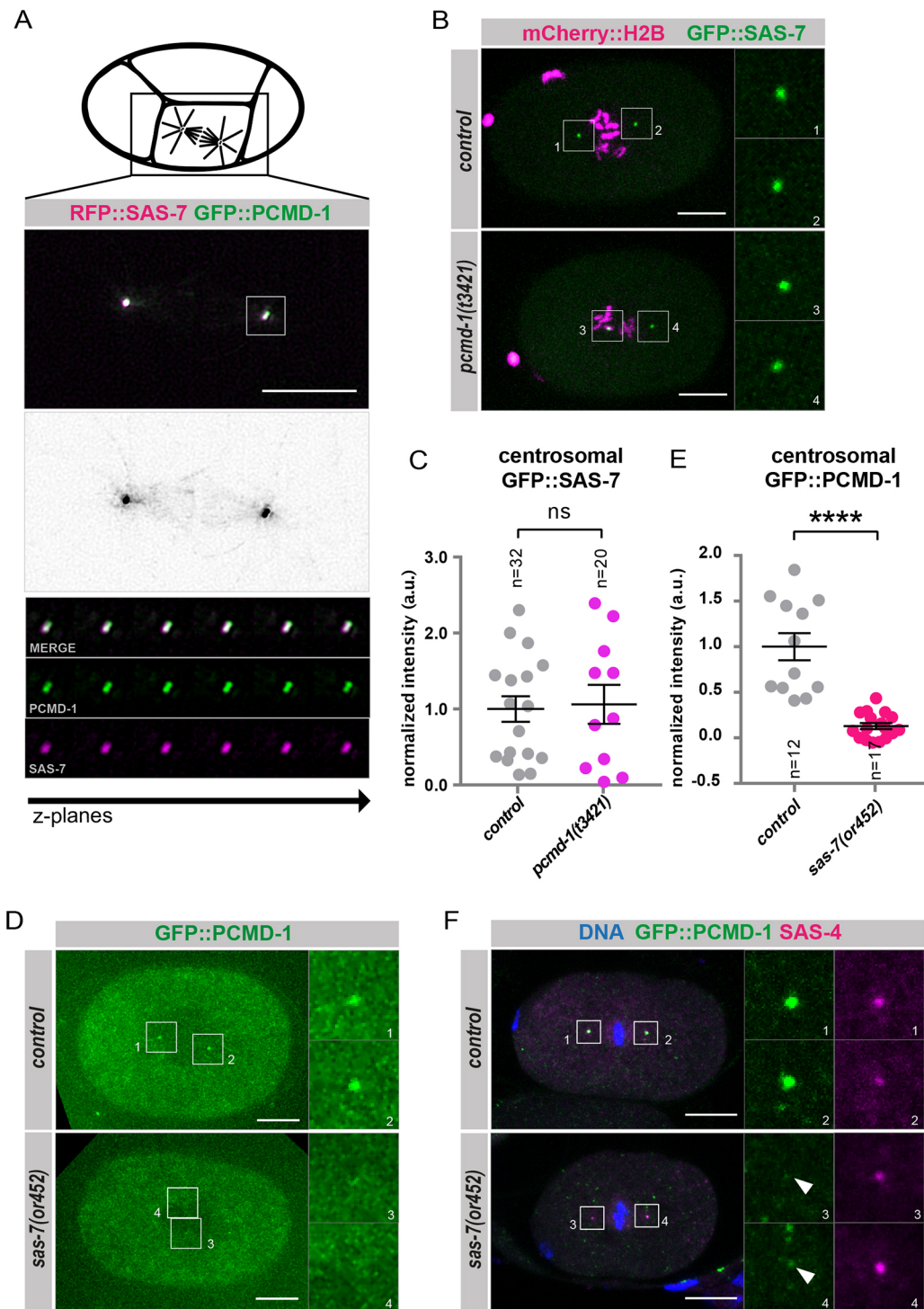E.Z., 0000-0003-1450-8684; T.M., 0000-0002-9449-3218

DEVELOPMENT

Fig. 1. SAS-7 recruits PCMD-1 to the centrioles. (A) Mitotic centrosomes of the EMS cell of a 4-cell embryo (schematic) expressing GFP::PCMD-1 and RFP::SAS-7 (*n*=6 centrosomes). Note that some GFP signals decorated astral and kinetochore microtubules of the mitotic spindle (middle panels). Lower panels represent a montage of different *z*-planes spanning a centriole pair. (B) Stills of time-lapse spinning disk confocal images of *mCherry::h2b;gfp::sas-7* (*n*=16) and *pcmd-1(t3421);mCherry::h2b;gfp::sas-7* (*n*=10) embryos during nuclear envelope break-down (NEB). Insets show centrosomes. (C) Normalized centrosomal GFP::SAS-7 signal intensities in control and *pcmd-1(t3421)* mutant embryos at NEB. Two-sample *t*-test, *n*=number of analyzed centrosomes. (D) Stills of time-lapse spinning disk confocal images of *gfp::pcmd-1* (*n*=6) and *gfp::pcmd-1;sas-7(or452)* (*n*=10) embryos during pronuclear meeting. Centrosome areas are shown enlarged for the GFP::PCMD-1 signal. (E) Normalized centrosomal GFP::PCMD-1 signal intensities in control and *sas-7(or452)* embryos at NEB. Two-sample *t*-test, *n*=number of analyzed centrosomes. (F) Representative confocal images of fixed *gfp::pcmd-1* (*n*=8) and *gfp::pcmd-1;sas-7(or452)* (*n*=11) one-cell embryos in prometaphase stained for DNA, GFP and SAS-4. Insets represent single channels of the centrioles. Arrowheads indicate the GFP::PCMD-1 signal. Error bars denote s.e.m. ****P<0.0001; ns, not significant (*P*>0.05). a.u., arbitrary units. Scale bars: 10 μm.

imaging of GFP::SAS-7 in *pcmd-1(t3421)* mutant embryos revealed that GFP::SAS-7 levels at centrioles are comparable to that of control embryos (Fig. 1B,C). We concluded that PCMD-1 is not involved in the recruitment of SAS-7 to the centrioles. To test inversely whether SAS-7 is required for PCMD-1 recruitment to the centrosome, we crossed an in-locus-tagged *gfp::pcmd-1* with *sas-7(or452)* mutant animals. Whereas GFP::PCMD-1 at the centrosome was apparent in all control embryos, the centrosomal GFP::PCMD-1 signal was significantly reduced in *sas-7(or452)* one-cell embryos (Fig. 1D,E). Interestingly, a GFP::PCMD-1 signal was consistently detected at sperm-derived *sas-7(or452)* centrioles during pronuclear migration (Fig. S1A). Shortly thereafter, this signal decreased close to the detection limit (Fig. 1E, Fig. S1A). As an alternative means to address the SAS-7-dependent localization of PCMD-1, we performed immunostaining using antibodies against GFP and SAS-4 to mark the centrioles. In one-cell control embryos, all centrosomal SAS-4 foci colocalized with a clear GFP::PCMD-1 signal (Fig. 1F). In contrast, only a very weak GFP::PCMD-1 signal was observed at SAS-4 foci in *sas-7(or452)* embryos (Fig. 1F), probably reflecting the hypomorphic nature of the *sas-7(or452)* allele (Sugioka et al., 2017). Note that centrosomal GFP::PCMD-1 signal was detectable in *sas-7(or452)* multicellular embryos (Fig. S1B). In these late embryos, PCMD-1 could be recruited through a SAS-7-independent mechanism, as is the case at the ciliary base (Garbrecht et al., 2021; Magescas et al., 2021). Thus, SAS-7 is necessary to maintain PCMD-1 at the centrosome during the first cell division.

PCMD-1 bridges centriolar and PCM scaffold proteins

The genetic dependency of PCMD-1 centrosomal localization on SAS-7 raises the possibility that PCMD-1 is recruited to the centriole by direct interaction with SAS-7. To determine whether PCMD-1 and SAS-7 interact with each other and with other centrosomal proteins such as SAS-4, SPD-2, SPD-5 and PLK-1, we performed a candidate-based yeast two-hybrid screen (Fields and Song, 1989). We generated bait plasmids containing the cDNAs of SAS-7 and PCMD-1 and prey plasmids for the candidate proteins SAS-4, SAS-7, PCMD-1, SPD-2, SPD-5 and PLK-1. The readouts of positive interactions were growth and the expression of a GFP reporter. We categorized proteins showing both readouts on day 3 as strong interactors and on day 5 as weak interactors.

Previous yeast two-hybrid screens identified SAS-7 as a binding partner of SPD-2 (Sugioka et al., 2017; Boxem et al., 2008; Li et al., 2004) and SAS-4 (Boxem et al., 2008). We used these interactions to validate our yeast two-hybrid assay. As previously reported, we found that SAS-7 interacts with SPD-2 and SAS-4 (Fig. 2A,B). However, we could not detect an interaction between SAS-7 and PCMD-1 using either protein as bait or prey. Therefore, we tested whether PCMD-1 could interact with the centriolar proteins SAS-4 or SPD-2. We observed strong interaction of PCMD-1 with SAS-4 but not with SPD-2. Next, we tested whether PCMD-1 could bind to the PCM scaffold protein SPD-5, the kinase PLK-1 or itself. We detected strong interaction of PCMD-1 with itself and a weaker interaction with SPD-5 and PLK-1. In turn, SAS-7 did not interact with SPD-5 or with PLK-1 (Fig. 2A,B).

To confirm the interactions between the PCMD-1 bait and SAS-4, PLK-1 and SPD-5 preys, we reversed bait and prey. Again, we observed that PLK-1 and SAS-4 interacted with PCMD-1 (Fig. 2C). Because SPD-5 bait autoactivated, we turned to an alternative assay to confirm this interaction. We expressed *C. elegans* PCMD-1 tagged with EGFP (EGFP::PCMD-1) and SPD-5 tagged with mCherry and 6xHis (mCherry::SPD-5::6xHis) in human HEK293T cells and

performed a co-immunoprecipitation. We successfully co-immunoprecipitated EGFP::PCMD-1 with SPD-5, confirming our yeast two-hybrid observation (Fig. 2D).

The yeast two-hybrid assay revealed no interaction of PCMD-1 with SAS-7 or SPD-2. However, both PCMD-1 and SAS-7 interact with SAS-4. Thus, rather than direct recruitment of PCMD-1 by SPD-2 or SAS-7, SAS-4 could theoretically act as a linker between PCMD-1 and SAS-7. However, in accordance with previous studies we found that in *sas-7(or452)* mutant embryos, where no PCMD-1 is found at the centrosome, SAS-4 foci are still present (Fig. 1F) (Sugioka et al., 2017). Therefore, it is highly unlikely that SAS-4 is accountable for the loss of PCMD-1 centrosomal localization in *sas-7(or452)* embryos.

In summary, PCMD-1 interacts with the centriolar protein SAS-4, the PCM protein SPD-5, the mitotic kinase PLK-1, and with itself. We propose that PCMD-1 acts as a functional bridge between the centrioles and the PCM scaffold.

PCMD-1 recruits SPD-5 and PLK-1 to an ectopic location

PCMD-1 is required to recruit SPD-5 to the centrosome (Erpf et al., 2019). This finding is strongly supported by our yeast-two hybrid interaction data, which indicates that PCMD-1 anchors the PCM scaffold to the centriole. Therefore, we investigated whether PCMD-1 is also able to recruit SPD-5 to an ectopic location. To address this, we established a 'translocation assay' by targeting PCMD-1 to an ectopic location in the cell and testing whether PCMD-1 is capable of recruiting SPD-5 to this cellular location. To tether PCMD-1 to the plasma membrane, we fused the mkate2::PCMD-1 reporter to the plcδ1PH-domain and expressed it under a heat-shock promoter. Upon heat shock, PH::mkate2::PCMD-1 was expressed and reliably translocated to the plasma membrane (Fig. 3A,B).

We tested whether membrane-bound PH::mkate2::PCMD-1 could recruit GFP::SPD-5 in the *pcmd-1(t3421)* mutant, which has a premature stop codon, and in the presence of wild-type PCMD-1. In *pcmd-1(t3421)* animals, recruitment of SPD-5 to the centrosome is compromised owing to the lack of endogenous PCMD-1 (Erpf et al., 2019). Therefore, more GFP::SPD-5 is expected in the cytoplasm. In control embryos without heat shock, GFP::SPD-5 was never detected at the plasma membrane. Induction of PH::mkate2::PCMD-1 by heat shock resulted in GFP::SPD-5 localization to the plasma membrane in 95.2% of the *pcmd-1(t3421)* and 68.4% of the wild-type embryos (Fig. 3B,C, Fig. S2A,B).

Because PLK-1 is also a PCM component and interacts with PCMD-1 in the yeast two-hybrid assay, we tested whether the in-locus-tagged PLK-1::sGFP translocates to the plasma membrane in a PCMD-1-dependent manner. Similar to GFP::SPD-5, PLK-1::sGFP localized to the plasma membrane in 41.4% of *pcmd-1(t3421)* and 26.3% of wild-type embryos after heat shock but did not localize to the membrane without heat shock (Fig. 3B,C, Fig. S2A, B). Note that the PLK-1::sGFP signal at the membrane was much weaker compared with the GFP::SPD-5 signal.

SPD-5 phosphorylation by PLK-1 is essential for PCM maturation (Woodruff et al., 2015). In the absence of PLK-1 phosphorylation at four specific residues, SPD-5 only forms a centrosome core but fails to assemble the mitotic scaffold. Therefore, we tested whether the translocation of SPD-5 to the membrane requires phosphorylation by PLK-1 at these residues. For this, we used a strain carrying RNAi-resistant GFP::SPD-5(4A), in which the four PLK-1 phosphorylation sites were substituted by alanine residues (Woodruff et al., 2015). To eliminate the endogenous SPD-5, embryos were treated with RNAi against *spd-5*. We found that GFP::SPD-5(4A) was still able to translocate
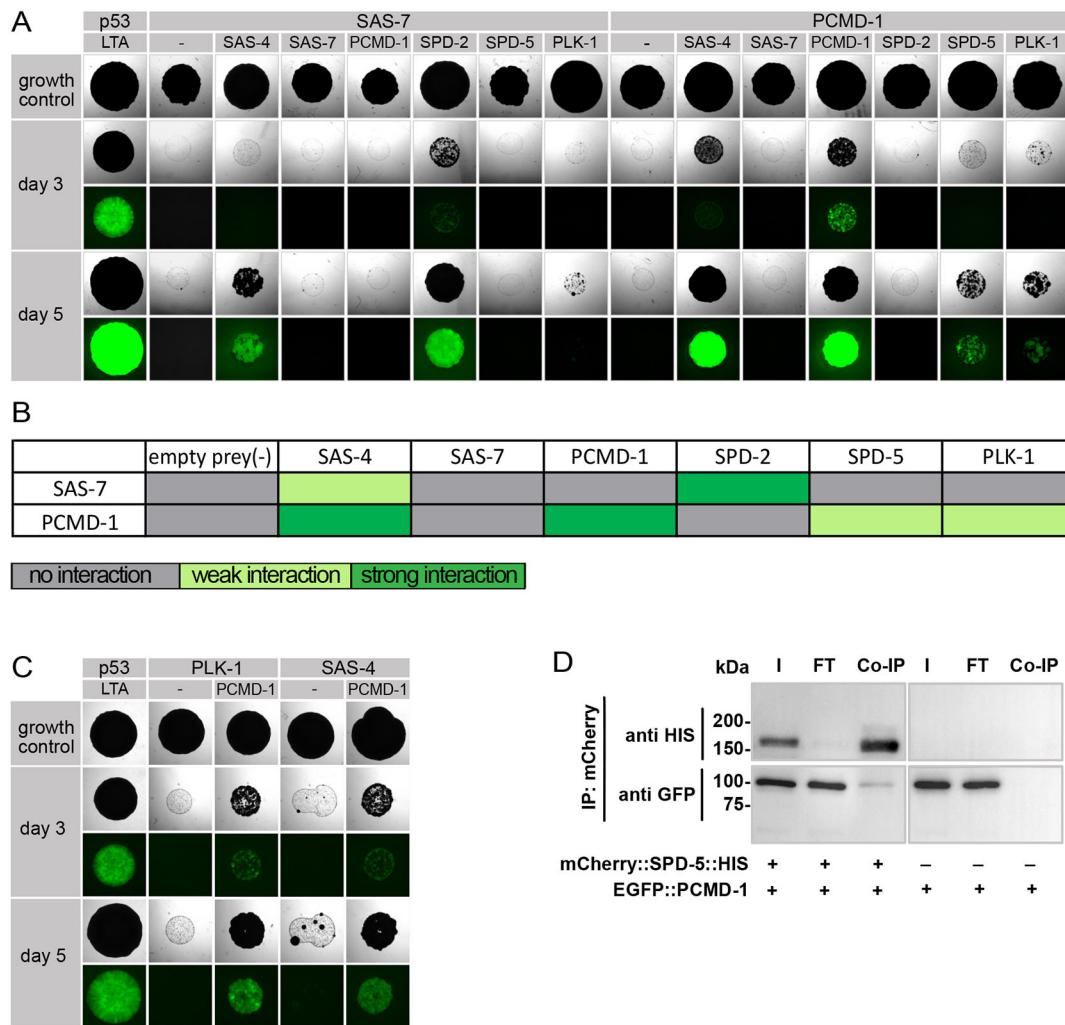
Fig. 2. PCMD-1 interacts with centriolar and PCM scaffold proteins. (A) Images of representative yeast two-hybrid colonies. Interaction of bait proteins SAS-7 and PCMD-1 with centrosomal proteins SAS-4, SAS-7, PCMD-1, SPD-2, SPD-5 and PLK-1 as preys, respectively. The top panel represents growth control, middle panels represent colonies screened on day 3 for growth on the selection medium and expression of the GFP-reporter, and the bottom panels represent colonies screened on day 5 for growth on the selection medium and expression of the GFP-reporter. (B) Summary of protein-protein interactions observed categorized by the strength of their interactions. (C) Images of representative yeast two-hybrid colonies. Interaction of bait proteins PLK-1 and SAS-4 with PCMD-1 prey. p53 with LTA was used as a positive control. (D) Co-immunoprecipitation of *C. elegans* EGFP::PCMD-1 and mCherry::SPD-5::6xHIS expressed in HEK293T cells using an RFP-trap. Co-IP, co-immunoprecipitation; FT, flow-through; I, input fraction.

efficiently to the membrane (96.8%; Fig. 3D,E), indicating that the membrane-bound GFP::SPD-5 pool does not resemble the mitotic PCM scaffold of SPD-5. Membrane translocation of PLK-1 could be mediated through SPD-5. To test this possibility, we performed the experiment in the *spd-5(RNAi)* background. PLK-1::sGFP recruitment still took place (45.9%; Fig. 3D,E). Thus, PCMD-1 can recruit PLK-1 independently of SPD-5.

Next, we tested whether PCMD-1 can also induce translocation of centriolar proteins. Interestingly, PH::mkate2::PCMD-1 was unable to translocate GFP::SAS-4, GFP::SAS-7 or GFP::PCMD-1 in any of the analyzed *pcmd-1(t3421)* embryos (Fig. 3B,C). This was unexpected, especially for SAS-4, because the interaction in the yeast two-hybrid assay was very strong. One explanation could be that a centriole tethering of SAS-4 prevents membrane translocation by PCMD-1. To test this hypothesis, we used a GFP::SAS-4 construct that lacks the conserved T complex protein 10 (TCP) domain, needed for its binding to SAS-5 (Cottee et al., 2013). When endogenous SAS-4 is eliminated by RNAi, the RNAi resistant GFP::SAS-4(ΔTCP) protein is not tethered to the centrioles but still

localizes to the PCM (Cottee et al., 2013) (Fig. S2C). In the translocation assay, PCMD-1 was unable to recruit GFP::SAS-4(ΔTCP) to the membrane (Fig. S2C,D), raising the possibility that the interaction between SAS-4 and PCMD-1 is not through the PCM pool and may require the local environment at the centrioles. Therefore, the ability of PCMD-1 to ectopically anchor proteins to the plasma membrane is specific to the PCM scaffold proteins SPD-5 and PLK-1. Alternatively, the deletion of the TCP domain could compromise the interaction between SAS-4 and PCMD-1.

PCMD-1 is recruited to the centrioles prior to SPD-5
Our findings suggest that PCMD-1 could recruit the initial PCM core to the PCM-less sperm centrioles in the *C. elegans* one-cell embryo. Therefore, we investigated whether PCMD-1 is loaded onto the sperm centrosomes before SPD-5. In the *C. elegans* zygote, SPD-5 is recruited to the sperm-derived centrioles after the completion of meiosis II of the female pronucleus and concomitant with the ability of the centrosome to nucleate microtubules (McNally et al., 2012). This paradigm allows us to
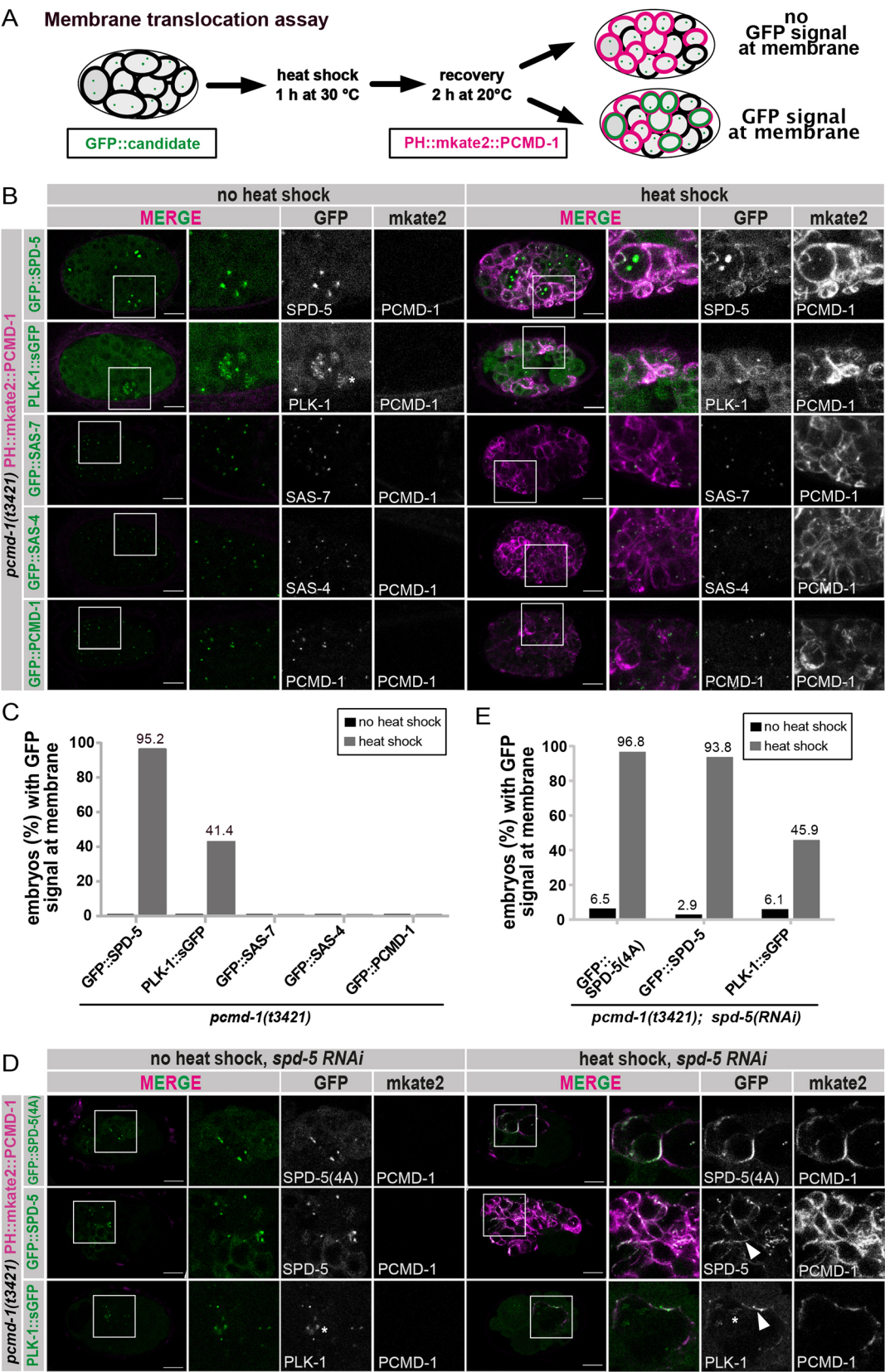
Fig. 3. See next page for legend.

investigate whether PCMD-1 is loaded to the centrioles prior to SPD-5 recruitment using marked mating experiments in which only the sperm or the oocyte expresses a fluorescent marker. First, we

tested whether paternal GFP::PCMD-1 could be detected at the centrosome after fertilization. For this, we mated *fog-2(q71)* females lacking sperms with GFP::PCMD-1-expressing males, thus labeling

DEVELOPMENT

5

Fig. 3. PCMD-1 targets SPD-5 and PLK-1 to the plasma membrane.
(A) Schematic of the 'translocation assay'. After 1 h heat shock to induce
expression and 2 h recovery, PH::mkate2::PCMD-1 is expressed and binds to
the plasma membrane of a multicellular embryo. If PH::mkate2::PCMD-1
recruits GFP-tagged candidate proteins, they will also localize to the plasma
membrane (bottom embryo). If PH::mkate2::PCMD-1 is not able to recruit, the
localization of the GFP-tagged candidate proteins will not change upon PH::
mkate2::PCMD-1 expression (top embryo). (B) Representative multicellular
embryos of the 'translocation assay' for GFP::SPD-5 (*n*=17 no heat shock;
n=21 heat shock), PLK-1::sGFP (*n*=21 no heat shock; *n*=29 heat shock), GFP::
SAS-7 (*n*=20 no heat shock; *n*=23 heat shock), GFP::SAS-4 (*n*=28 no heat
shock; *n*=28 heat shock) and GFP::PCMD-1 (*n*=25 no heat shock; *n*=27 heat
shock) fusion proteins in the *pcmd-1(t3421)* background with and without heat
shock. Selected regions (boxed) are enlarged and shown as merge and single
channels. Note that PLK-1::sGFP signal at the plasma membrane is less
intense than GFP::SPD-5. Scale bars: 10 μm. (C) Quantification of B showing
the percentage of embryos with GFP signal at the membrane after heat shock in
the *pcmd-1(t3421)* background. (D) Representative multicellular embryos
of the 'translocation assay' using GFP::SPD-5 (*n*=31 no heat shock; *n*=31 heat
shock), GFP::SPD-5(4A) (*n*=34 no heat shock; *n*=32 heat shock) and PLK-1::
sGFP (*n*=33 no heat shock; *n*=37 heat shock) in a *pcmd-1(t3421);spd-5(RNAi)*
background. Selected regions (boxed) are enlarged and shown as merge and
single channels. Arrowheads indicate the membrane-localized GFP signal.
Asterisks indicate kinetochore localization of PLK-1::sGFP. Scale bars: 10 μm.
(E) Quantification of D showing the percentage of embryos with GFP signal at
the membrane after heat shock in the *pcmd-1(t3421); spd-5(RNAi)*
background.

sperm centrioles (Fig. S3A) (Erpf et al., 2019). We could not detect
GFP::PCMD-1 at centrioles in any of the analyzed embryos after the
completion of meiosis II. Second, we mated GFP::PCMD-1
females, treated with *fem-1(RNAi)* to block sperm production,
with control *fog-2(n71)* males with unlabeled sperm centrioles. We
found that the GFP::PCMD-1 signal was detected at the
centrosomes in all analyzed embryos during the first mitotic
division (Fig. S3C). These results suggest that sperm-derived
PCMD-1 is not maintained and that the maternal PCMD-1 is
recruited to the centrioles after fertilization.

To determine exactly when maternal PCMD-1 is recruited to the
centriole after fertilization and to temporally map its loading with
respect to SPD-5, we immunostained embryos from GFP::PCMD-1
females mated with males with unlabeled sperm centrioles
(Fig. S3C,D), using antibodies against SPD-5 and GFP. In
meiosis I embryos, neither GFP::PCMD-1 nor SPD-5 foci were
present at the centrioles (Fig. S3E), indicating that maternal
GFP::PCMD-1 was not yet incorporated in the centrioles. During
meiosis II, we found that a GFP::PCMD-1 focus, without any
detectable SPD-5, was visible at 90.5% of sperm centrioles
(Fig. S3D,E). In the remaining 9.5% of embryos, categorized as
early meiosis II, neither GFP::PCMD-1 nor SPD-5 foci were present
(Fig. S3D). Therefore, we conclude that maternal GFP::PCMD-1 is
recruited to the sperm centrioles at meiosis II. After meiosis II, when
sperm pronuclei are decondensed, SPD-5 colocalized with
GFP::PCMD-1 at the centrosomes in 87% of the embryos
(Fig. S3D,E). We never observed embryos with centrosomes only
labeled by SPD-5.

In summary, our results are consistent with a model in which
maternal GFP::PCMD-1 is recruited to the sperm-derived centrioles
shortly after fertilization and subsequently recruits SPD-5 and
PLK-1 to form the centrosome core. These findings strengthen the
hypothesis that PCMD-1 bridges centriolar and PCM proteins.

The coiled-coil domain promotes PCMD-1 loading to the centrosome and self-interaction

To determine how PCMD-1 is anchored to the centrosome, we
next examined which part of the protein is necessary for its

centrosomal targeting. PCMD-1 is predicted to have a single coiled-
coil domain and six intrinsically disordered regions (IDRs 1-6),
which partially overlap with low complexity regions (Fig. 4A)
(UniProt Consortium, 2019; Schultz et al., 2000; Letunic and
Bork, 2018). Coiled-coil domains often mediate protein-protein
interactions, including oligomerization, and these interactions can
have regulatory functions for centrosomal proteins (Leidel et al.,
2005; Kitagawa et al., 2011; Qiao et al., 2012; Hilbert et al.,
2013; Lettman et al., 2013; Rogala et al., 2015). Therefore, we
set out to investigate the function of the coiled-coil domain
in PCMD-1.

To examine the function of the coiled-coil domain, we deleted the
sequence from E86 up to and including F118, predicted as the
coiled-coil domain by the COILS program (Lupas et al., 1991;
Lupas, 1996), using CRISPR/Cas9 in the in-locus-tagged GFP::
PCMD-1 protein. We refer to this deletion as *gfp::pcmd-1(ΔCC)*
(Fig. 4A). In a lethality test, 97.5% of the *gfp::pcmd-1* embryos and
87.6% of the *gfp::pcmd-1(ΔCC)* embryos survived at 25°C
(Fig. 4B). Thus, the deletion of the predicted coiled-coil domain
compromised viability.

Next, we investigated whether the GFP::PCMD-1(ΔCC) protein
could localize to the centrosome. We performed live-cell imaging on
worms expressing GFP::PCMD-1 and GFP::PCMD-1(ΔCC).
Whereas GFP::PCMD-1 efficiently localized to the centrosomes in
all analyzed embryos, the GFP::PCMD-1(ΔCC) signal on average
appeared much weaker (Fig. 4C, Movies 1 and 2). Measuring the
mean centrosomal GFP signal intensity confirmed that PCMD-1
without the coiled-coil domain was significantly reduced at the
centrosomes in comparison with wild-type PCMD-1, whereas
cytoplasmic levels remained unchanged (Fig. 4D,E). Thus, the
coiled-coil domain is necessary for efficient centrosomal loading of
PCMD-1 but is not essential for the viability of the embryos. Given
that coiled-coil domains are often implicated in the oligomerization
of centrosomal proteins, we asked whether PCMD-1 self-interaction
was compromised in the absence of the coiled-coil domain. To this
end, we expressed PCMD-1(ΔCC) as a bait plasmid and probed
its interaction with the PCMD-1(ΔCC) prey (Fig. 4F). In the absence
of the coiled-coil domain, PCMD-1 self-interaction was lost
(Fig. 4F).

This raises the question of how embryos with reduced centrosomal
PCMD-1 levels can divide. To investigate whether these animals
could still recruit the PCM scaffold, we immunostained GFP::
PCMD-1(ΔCC) embryos using antibodies against GFP and SPD-5
and performed live-cell imaging of RFP::SPD-5. We found that
SPD-5 was still recruited to the centrosome in all analyzed embryos,
even in embryos in which GFP::PCMD-1(ΔCC) was almost
undetectable (Fig. 4G, Fig. S4A). Although overall centrosomal
RFP::SPD-5 levels remained similar to the control embryos in the
absence of the coiled-coil domain (Fig. S4A,B), the SPD-5
centrosome matrix appeared to be much more dispersed and
disorganized (Fig. 4G). To quantify the degree of disorganization,
we measured centrosome circularity using immunofluorescence
staining and found that mean centrosome circularity values were
significantly lower in *gfp::pcmd-1(ΔCC)* embryos (Fig. 4H).

We propose that the coiled-coil domain facilitates PCMD-1 self-
interaction and thereby promotes efficient PCMD-1 accumulation at
the centrosome and the maintenance of PCM scaffold integrity.

Regions in the C-terminal part of PCMD-1 target the protein to the centrosome and cilia

The fact that GFP::PCMD-1(ΔCC) could still be recruited to the
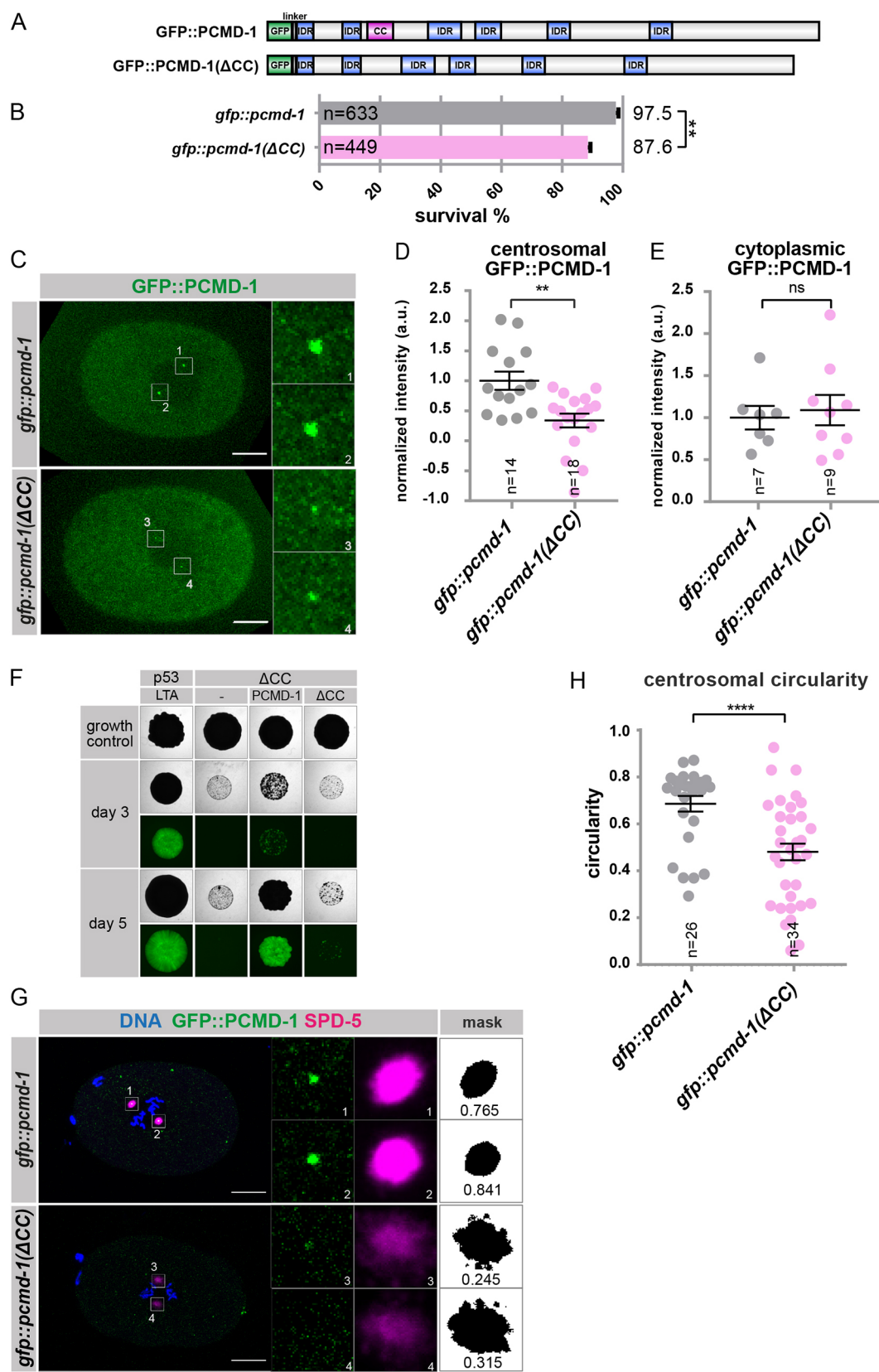centrosome indicates that protein regions other than the coiled-coil

DEVELOPMENT

6

Fig. 4. See next page for legend.

domain might play a role in centrosomal anchoring. To map which part of the protein is involved, we used a previously established single-copy replacement system (Erpf et al., 2019). *pcmd-1(t3421)* mutant animals carry a stop codon before the coiled-coil domain and are lethal at 25°C (Fig. S5A). Reconstituting a single copy of the PCMD-1 cDNA under the regulatory elements of the *mai-2* gene

Fig. 4. The coiled-coil domain promotes PCMD-1 accumulation at the centrosome and PCM scaffold integrity. (A) Top: Schematic of the domain structure of endogenously tagged GFP::PCMD-1 protein (aa 2-630), with predictions of the coiled-coil domain (CC) and six IDRs. Bottom: Schematic of the domain structure of a truncated version, with the deleted coiled-coil domain (Δ86-117). All domains except GFP are represented on a relative scale. (B) Survival of gfp::pcmd-1 and gfp::pcmd-1(ΔCC) animals at 25°C. P-values were calculated by Mann–Whitney U-Test, n=number of analyzed embryos. (C) Stills of time-lapse imaging of gfp::pcmd-1 (n=7) and gfp::pcmd-1(ΔCC) (n=9) embryos at NEB. Centrosomal areas were determined by DIC imaging and are shown enlarged for the GFP::PCMD-1 signal. See Movies 1 and 2. (D) Normalized centrosomal GFP signal intensities in embryos expressing gfp::pcmd-1 and gfp::pcmd-1(ΔCC) at NEB. P-values were calculated by Mann–Whitney U-test. n=number of analyzed centrosomes. (E) Normalized cytoplasmic GFP signal intensities in embryos expressing gfp::pcmd-1 and gfp::pcmd-1(ΔCC) at NEB. P-values were calculated by two-sample t-test. n=number of analyzed embryos. (F) Images of representative yeast two-hybrid colonies. Interaction of bait proteins PCMD-1(ΔCC) with PCMD-1 and PCMD-1(ΔCC) as preys. p53 with LTA was used as a positive control. (G) Representative images of fixed embryos of the indicated genotype stained for DNA, GFP and SPD-5. Centrosomes are enlarged in individual channels and the corresponding masks of the SPD-5 signal. Values of centrosomal circularity are indicated. (H) Quantification of SPD-5 circularity in gfp::pcmd-1 and gfp::pcmd-1(ΔCC) embryos. P-values were calculated by Mann–Whitney U-Test, n=number of analyzed centrosomes. Error bars denote s.e.m. **$P<0.01$, ****$P<0.0001$; ns, not significant ($P>0.05$). a.u., arbitrary units. Scale bars: 10 μm.

rescues survival rates to 96.2% (Fig. S5A). We used this assay to test the functionality and localization of different truncations of the PCMD-1 protein. GFP::PCMD-1(N) spans the region E2-N117, including the first two IDRs and the coiled-coil domain. GFP::PCMD-1(C) comprises amino acids F118 to the stop codon, spanning the remaining IDRs (Fig. 5A). In the survival assay, GFP::PCMD-1(C) could rescue the lethality of pcmd-1(t3421) to 90.8% survival, whereas GFP::PCMD-1(N) was not sufficient to rescue viability (0.3%) (Fig. S5A). Interestingly, GFP::PCMD-1(N) even had a dominant-negative effect on the viability of pcmd-1(t3421) at the permissive temperature of 15°C, reducing it from 41% to 28% (Fig. S5B).

Next, we assessed the ability of these constructs to localize to the centrosome by live-cell imaging. Centrosomal GFP signal was detected in all GFP::PCMD-1(C) embryos, albeit with slightly reduced GFP signal intensities compared with control animals (Fig. 5B,C). In contrast, we could not detect any GFP signal at the centrosome in embryos expressing the GFP::PCMD-1(N) constructs, even though the cytoplasmic levels were much higher (Fig. 5B, Fig. S5C). Therefore, the C-terminal part of PCMD-1, excluding the coiled-coil domain and IDR1 and IDR2, is sufficient for PCMD-1 anchoring to the centrosome.

To further map the part of PCMD-1 that targets the protein to the centrosome, we subdivided the C-terminal part into two fragments spanning F118-D342 (C1) and G343-stop codon (C2) (Fig. 5A). In the survival assay, neither GFP::PCMD-1(C1) nor GFP::PCMD-1(C2) rescued the lethality of pcmd-1(t3421) (Fig. S5A). However, GFP::PCMD-1(C2) still localized to the centrosome, whereas GFP::PCMD-1(C1) did not (Fig. 5B,C). This raises the possibility that the C2 part of the PCMD-1 could be interacting with SAS-4. Therefore, we expressed the PCMD-1(C2) as a bait together with SAS-4 as a prey in the yeast two-hybrid assay (Fig. 5D). The PCMD-1(C2) bait strongly interacted with the SAS-4 prey. A similarly strong interaction was detected between the SAS-4 bait and the PCMD-1(C2) prey (Fig. 5D).

Similar to the centrosomes in the embryo, only GFP::PCMD-1, GFP::PCMD-1(C) and GFP::PCMD-1(C2) localized to the ciliary

base of adult animals (Fig. S6). In particular, signals from GFP::PCMD-1(C) and GFP::PCMD-1(C2) appeared stronger than the control, extending along the cilia (Fig. S6).

In pcmd-1(t3421) mutant animals, SPD-5 recruitment to the centrosome is severely compromised (Erpf et al., 2019). Therefore, we tested whether the truncated parts of PCMD-1 that localize to the centrosome can restore SPD-5 recruitment. In animals expressing GFP::PCMD-1(C), levels of RFP::SPD-5 at metaphase were similar to those in animals carrying the full-length GFP::PCMD-1. However, in GFP::PCMD-1(C2)-expressing animals, RFP::SPD-5 levels were largely reduced (Fig. S5C,D). Thus, the C2 part of PCMD-1, including IDR6, is sufficient to target PCMD-1 to the centrosome but is insufficient to recruit the PCM scaffold composed of SPD-5.

The fact that PCMD-1(C2) strongly localizes to the centrosome prompted us to test a construct that lacks the C2 part (GFP::PCMD-1(ΔC2) E2-D342). Surprisingly, GFP::PCMD-1(ΔC2) could still localize to the centrosome, although the centrosomal levels were reduced by 60% in comparison with the full-length construct (Fig. 5B,C). However, GFP::PCMD-1(ΔC2) fully rescued the viability of pcmd-1(t3421) and recruited RFP::SPD-5 to the centrosome (Fig. S5A,D,E).

Intriguingly, we could not detect GFP::PCMD-1(ΔC2) at the cilia, indicating that the C2 part is absolutely essential for ciliary base targeting (Fig. S6). Given that the C2 part contains IDR6, we generated a worm strain that expresses GFP::PCMD-1(ΔC2.2) E2-G514, a construct in which IDR6 is included. Centrosomal GFP::PCMD-1(ΔC2.2) levels were comparable to GFP::PCMD-1(ΔC2); however, the ciliary targeting was restored (Fig. S6).

In summary, multiple parts of PCMD-1 contribute to the centrosomal localization of PCMD-1. The PCMD-1(C2) region can bind SAS-4 and is sufficient for anchoring to the centrosome. The N-terminal construct lacking C2 can still localize to the centrosome, suggesting the presence of a second centrosome targeting region. The centrosomal PCMD-1(C2) is insufficient to recruit SPD-5 and for embryonic development. By contrast, the N-terminal construct lacking the C2 localizes to the centrosome at largely reduced levels and can restore centrosomal SPD-5 levels and function. The C2 part, and specifically the amino acids between D342 and G514 encompassing IDR6, are necessary for cilia localization.

DISCUSSION

In this study, we examine the mechanism by which PCMD-1 anchors the PCM scaffold to the centriole. We demonstrate that PCMD-1 interacts with the PCM scaffold protein SPD-5, the mitotic kinase PKL-1 and the centriolar protein SAS-4. Furthermore, tethering PCMD-1 at an ectopic cellular location is sufficient to recruit SPD-5 and PKL-1. In turn, the centrosomal localization of PCMD-1 depends on the outer centriolar protein SAS-7. Together with previous findings that PCMD-1 is required for SPD-5 recruitment to the PCM core in the one-cell embryo, these findings place the function of PCMD-1 between the centrioles and the PCM.

Our analysis revealed that PCMD-1 interacts with SPD-5. A similar protein-protein interaction has been established for pericentrin/Plp, the putative homolog of PCMD-1, and CDK5RAP2/Cnn the functional homolog of SPD-5 in vertebrates and Drosophila, respectively (Buchman et al., 2010; Lerit et al., 2015; Galletta et al., 2016). This interaction is especially important in C. elegans for the initial formation of the PCM core in the one-cell embryo. Paternally contributed centrioles in the one-cell embryo are deficient of the PCM core. SPD-5, which renders the
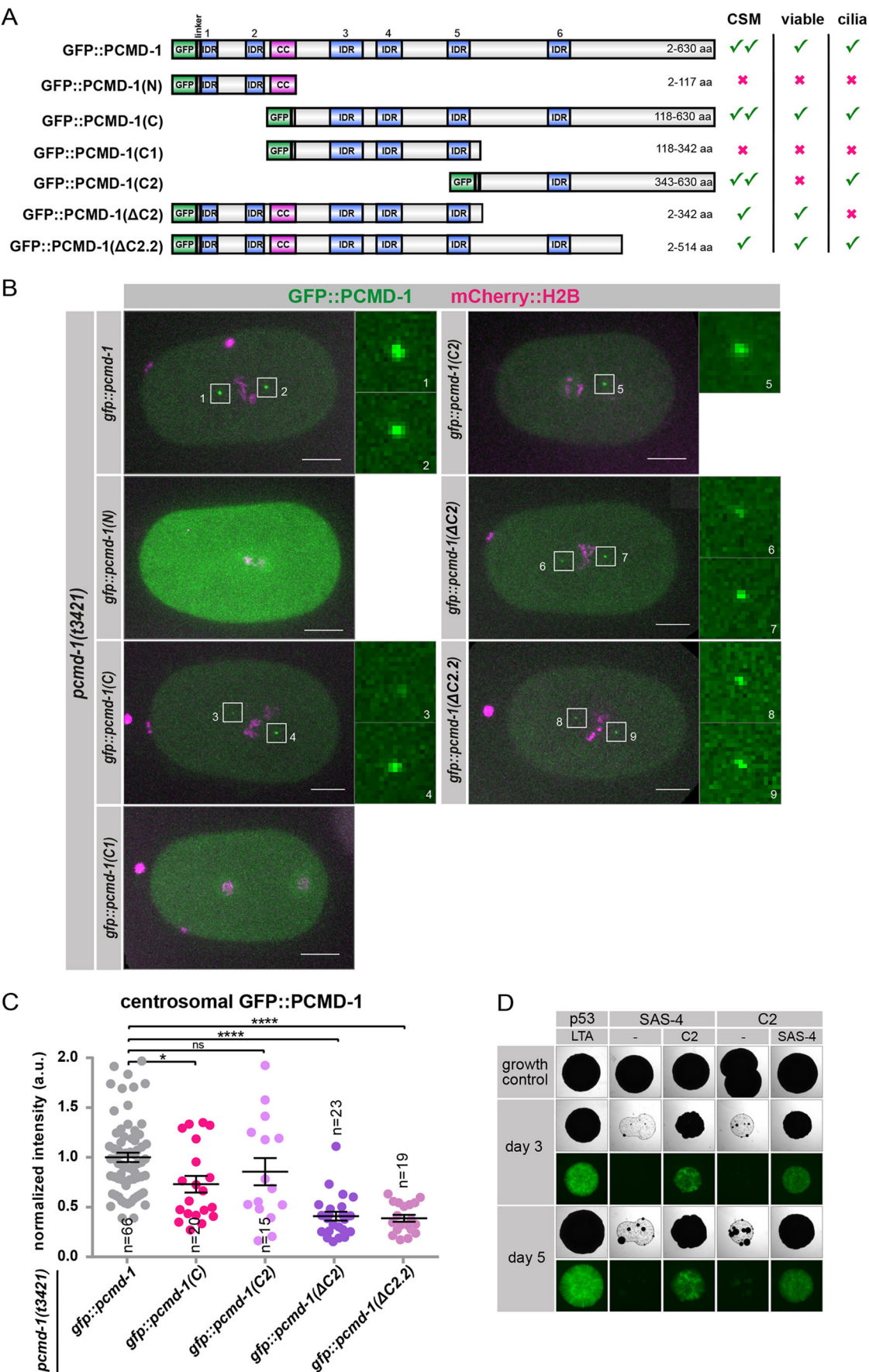
Fig. 5. See next page for legend.

Fig. 5. The C-terminal region targets PCMD-1 to the centrosome and binds SAS-4. (A) Domain structure of different GFP-tagged PCMD-1 constructs. All domains except GFP are represented to a relative scale. All constructs are expressed under the regulatory elements of the *mai-2* gene. Summary of localization and viability. CC, coiled-coil domain; CSM, centrosome. (B) Stills of time-lapse imaging of embryos expressing *gfp::pcmd-1* (*n*=12), *gfp::pcmd-1(N)* (*n*=7), *gfp::pcmd-1(C)* (*n*=10), *gfp::pcmd-1(C1)* (*n*=8), *gfp::pcmd-1(C2)* (*n*=9), *gfp::pcmd-1(ΔC2)* (*n*=12) and *gfp::pcmd-1(ΔC2.2)* (*n*=10) in combination with the *mCherry::h2b* in the *pcmd-1(t3421)* background at NEB. Enlarged are the two centrosomes. *n*=number of embryos. (C) Normalized centrosomal GFP signal intensities of embryos represented in B. *P*-values were determined for multiple comparisons with Kruskal–Wallis test and post-hoc Dunn's test adjusted with Holm correction; *n*=number of analyzed centrosomes. (D) Images of representative yeast two-hybrid colonies. Interaction of bait proteins SAS-4 and PCMD-1(C2) with SAS-4 and PCMD-1(C2) as preys. Error bars denote s.e.m. *$P<0.05$, ****$P<0.0001$; ns, not significant ($P>0.05$). a.u., arbitrary units. Scale bars: 10 μm.

centrioles' microtubule-organizing activity, is recruited from the maternal pool after female meiosis (McNally et al., 2012). Our findings that PCMD-1 is associated with centrioles prior to SPD-5 recruitment and that tethering of PCMD-1 at the plasma membrane is sufficient to recruit SPD-5 suggest that PCMD-1 is needed for SPD-5 accumulation and the formation of the PCM core after fertilization. In the translocation assay, PCMD-1 was consistently more effective at recruiting SPD-5 and PLK-1 to the plasma membrane in the absence of an endogenous PCMD-1. In the *pcmd-1(t3421)* mutant background, SPD-5 and PLK-1 are not efficiently recruited to the centrosome and are expected to be more abundant in the cytoplasm. This finding suggests a 'tug-of-war' between the centrosomal and membrane-bound PCMD-1 pools for the recruitment of SPD-5 and PLK-1. Membrane-bound PCMD-1 can also efficiently recruit a phospho-deficient version of SPD-5 in which the four residues that are phosphorylated by PLK-1 and that play a key role in the expansion and maturation of the mitotic PCM scaffold are mutated (Woodruff et al., 2015). Therefore, we speculate that PLK-1 phosphorylation of these residues is not required for PCMD-1 to recruit SPD-5 and that the membrane-targeted SPD-5 is analogous to the PCM core. The fact that PLK-1 can be translocated to the membrane in the absence of SPD-5 confirms our previous findings that PCMD-1 contributes to the formation of the PLK-1 pool at the centrosome independently of SPD-5 (Erpf et al., 2019). By bringing together PLK-1 and SPD-5, PCMD-1 facilitates the initiation of the centrosome maturation process.

In contrast to the PCM proteins, PCMD-1 was unable to relocate itself and the centriolar proteins SAS-4 and SAS-7 to the plasma membrane. This is consistent with observations that the centriolar localization of both SAS-4 and SAS-7 is independent of PCMD-1 (this study; Erpf et al., 2019). At the same time, this is puzzling especially in the case of PCMD-1 and SAS-4, for which we found a strong protein-protein interaction in the yeast two-hybrid system. Assays such as the yeast two-hybrid system do not indicate exactly where and when these interactions occur. In the case of PCMD-1, this could be due to a stronger binding of PCMD-1 to other centrosomal proteins, which prevent delocalization.

The fact that PCMD-1 could not recruit SAS-4(ΔTCP) raises the possibility that the PCMD-1/SAS-4 interaction may need a specific local environment or modification, which is provided at the centrioles but is absent at the cytoplasmic pool of the proteins. As the TCP domain of SAS-4 associates with SAS-5 and the centrioles, SAS-4(ΔTCP) only represents the PCM fraction of SAS-4 (Cottee et al., 2013). Even though we cannot exclude the formal possibility

that the deletion of the TCP domain additionally disrupts the interaction with PCMD-1, we consider it highly unlikely. We favor the possibility that either another protein bridges SAS-4 and PCMD-1 or that the proteins are post-translationally modified in the yeast two-hybrid system and at the centrosome, but not on the plasma membrane.

The outer centriolar protein SAS-7 is genetically upstream and required for PCMD-1 centrosomal recruitment in the one-cell embryo. This interaction could be direct or mediated through the known SAS-7 binding partners SPD-2 and SAS-4 (Sugioka et al., 2017). It has been shown previously that SAS-7 recruits SPD-2 to the centrosome, and that SAS-7 and PCMD-1 do not rely on a functional SPD-2 for their centrosomal localization (Sugioka et al., 2017; Erpf et al., 2019). In the yeast two-hybrid assay, PCMD-1 did not interact with SAS-7 or SPD-2. Thus, SPD-2 is an unlikely mediator of this interaction. As both PCMD-1 and SAS-7 interact with SAS-4 in the yeast two-hybrid assay, one could assume that the interaction is mediated through SAS-4. The absence of a fully formed daughter centriole in *sas-4(RNAi)* embryos does not allow us to make a conclusion about the requirement of SAS-4 for PCMD-1 localization. However, SAS-4 foci are still present in *sas-7(or452)* mutant embryos (Sugioka et al., 2017), in which little or no PCMD-1 is found at the centrosome. Although we cannot exclude the formal possibility that in *sas-7(or452)* mutant embryos SAS-4 changes its conformation or lacks a post-translational modification, which would hinder the interaction with PCMD-1, we do not favor a model in which SAS-4 is the only anchor for PCMD-1 on the centriole. We suggest that the interaction between SAS-7 and PCMD-1 is either indirect, through an unknown protein or an additional co-factor, or that a modification is required for interaction in the yeast two-hybrid and translocation assay. Structurally intact paddlewheels, which are altered in *sas-7(or452)* mutant animals, might be a prerequisite for PCMD-1 anchoring (Sugioka et al., 2017).

The presence of multiple IDRs in PCMD-1 suggests high conformational plasticity of the protein (Uversky, 2019). Our structure-function analysis revealed that multiple regions of PCMD-1 contribute to centrosomal targeting. The PCMD-1(C2) fragment, including IDR6, is sufficient for the centrosomal localization of PCMD-1. In the yeast two-hybrid assay, the same fragment strongly interacts with SAS-4, suggesting an interaction site with the centrioles (Fig. 6A). At the same time, centrosomal SPD-5 levels in the PCMD-1(C2) background are highly reduced and are comparable to the *pcmd-1(t3421)* mutants (Erpf et al., 2019). Thus, the PCMD-1(C2) fragment alone is insufficient to recruit SPD-5 and as a result does not support embryonic development. Therefore, we suggest that N-terminal parts of the protein are needed for SPD-5 recruitment and function (Fig. 6A). In accordance with this, constructs lacking the C-terminal region [PCMD-1(ΔC2) and PCMD-1(ΔC2.2)], which localize to the centrosome at much-reduced levels, are sufficient to accumulate SPD-5 and sustain viability.

The coiled-coil domain and IDR1 and IDR2 alone are insufficient for centrosomal targeting. Combination with the adjacent IDRs 3-5 restores localization and function. Therefore, the PCMD-1(C1) fragment reconstitutes major functional units. The dominant-negative effect on the viability of the coiled-coil domain and IDR1 and IDR2 could be explained by binding or sequestration of PCMD-1 interaction partners. In the context of the full-length protein, the coiled-coil domain significantly contributes to the accumulation of PCMD-1 at the centrosome and is required to form an organized PCM. The fact that the deletion of the coiled-coil
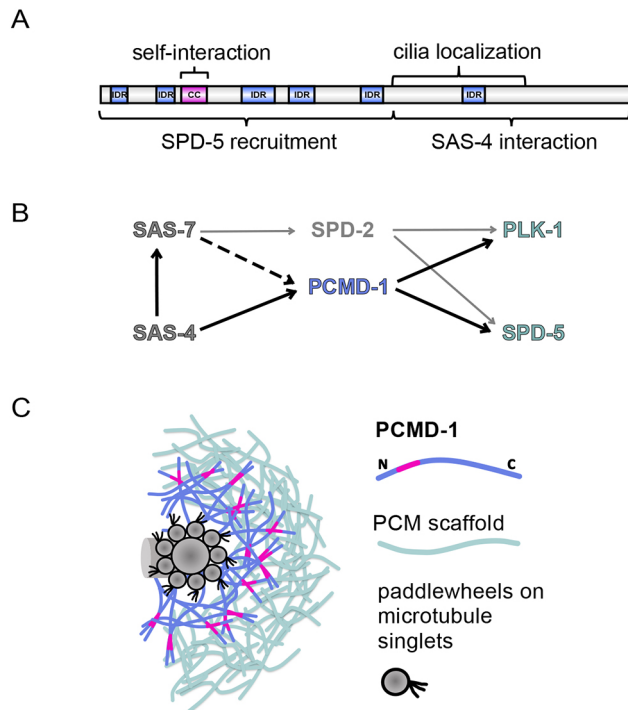
Fig. 6. Model of how PCMD-1 bridges the centrioles and PCM. (A) Structure of PCMD-1 with interaction sites indicated. CC, coiled-coil domain. (B) Genetic interactions of PCMD-1. PCMD-1 is genetically downstream of SAS-7 and SAS-4. SAS-7 itself interacts with SAS-4 and SPD-2. PCMD-1 acts genetically upstream of SPD-5 and PLK-1. Proteins other than PCMD-1, such as SPD-2, are involved in SPD-5 and PLK-1 recruitment to the centrosome. Interactions identified in this study are indicated by black arrows. Dashed arrow indicates genetic dependency. Gray arrow indicates interactions found in other studies. (C) Proposed model: PCMD-1 interacts with both centriolar and PCM proteins and thereby bridges the two centrosomal components. PCMD-1 is tethered to the centrioles through its C-terminal region, whereas the N-terminal region, including the coiled-coil domain (pink section), plays a role in PCMD-1 self-interaction and PCM formation.

domain only partially compromises viability is not surprising given that even the complete absence of an expanded SPD-5 scaffold at mitosis does not affect the viability (Woodruff et al., 2015). In animals with the deleted coiled-coil domain, SPD-5 levels are not altered, but the PCM appears more dispersed. This could be a direct effect of the coiled-coil domain on SPD-5 or an indirect effect as a result of the reduced PCMD-1 levels at the centrosome. In the yeast two-hybrid assay, we identified a strong self-interaction of PCMD-1, pointing to a tendency towards dimerization or formation of higher-order structures. Self-association is frequently found in centrosomal proteins. This has also been demonstrated for Plp in flies (Galletta et al., 2016). The self-interaction is abolished in the absence of the coiled-coil domains in both bait and prey but not when the coiled-coil domain is only deleted in the bait. This might indicate that PCMD-1/PCMD-1 self-interaction is mediated through binding of the coiled-coiled domain to a different part of the protein, rather than a dimerization of the coiled-coil domain. We speculate that the self-interaction of PCMD-1 plays a significant role in the PCM scaffold integrity. It would be interesting to investigate how exactly the physical properties of the mitotic PCM change in the absence of the coiled-coil domain of PCMD-1.

Recently it was shown that PCMD-1 and SPD-5 play an important role in the function of sensory cilia (Garbrecht et al., 2021; Magescas

et al., 2021). After initial recruitment, PCMD-1 and SPD-5 maintain each other at the ciliary base through a positive-feedback loop (Garbrecht et al., 2021). Through our structure-function analysis, we could separate the cilia localization of PCMD-1 from the centrosome localization. A part of the C2 region, missing in PCMD-1(ΔC2) but present in PCMD-1(ΔC2.2) restores PCMD-1 at the ciliary base (Fig. S6). Interestingly, this region comprises the most C-terminal IDR (IDR6), suggesting a potential role in targeting the C2 construct to the cilia. Our observation that PCMD-1 localizes to astral and spindle microtubules (Fig. 1A), could indicate binding to microtubules or a microtubule-binding protein. The enhanced localization of the GFP::PCMD-1(C2) along the length of the cilium may reflect increased microtubule binding, which in the cilia is limited by the N-terminal region in the full-length PCMD-1.

Together we propose a model (Fig. 6B,C) in which PCMD-1 is recruited to the centriole via two anchor points: SAS-7, either directly or indirectly, and SAS-4. The C-terminal part, especially the C2 part of PCMD-1, is sufficient for its centrosomal recruitment and interacts with SAS-4. We speculate that SAS-4 acts in parallel to SAS-7 and that this interaction needs the local environment at the centrioles. Centrosomal PCMD-1 recruits SPD-5 through its N-terminal parts, including IDR3-5. By bringing together SPD-5 and PLK-1, PCMD-1 facilitates PCM core formation and PCM maturation. The coiled-coil domain enhances PCMD-1 centrosomal accumulation through its self-interaction and contributes to the stabilization of the mitotic PCM scaffold. Given that proteins other than PCMD-1, such as SPD-2, play a role in SPD-5 scaffold formation during mitosis, this model might be cell-cycle specific or needed for the initial recruitment of SPD-5 to the PCM core. In summary, we propose that PCMD-1 is one of the proteins that anchors the PCM to the centrioles and functionally bridges the two centrosomal components.

MATERIALS AND METHODS
C. elegans strains maintenance
Worms were maintained on NGM plates seeded with the OP50 *Escherichia coli* strain under standard conditions at 15°C (Brenner, 1974). All worm strains used in this work are listed in Table S1. Unless indicated otherwise, for experimental use, progeny of worms shifted to 25°C at the L4 stage for 16-20 h, were analyzed. *gfp::pcmd-1; sas-7(or452)/hT2* worms were allowed to lay eggs for 3 h at 25°C. The laid eggs developed into adults at 25°C for 68 h. Progeny of *gfp::pcmd-1;sas-7(or452)* worms were used for further analysis.

Worm strain generation
Worms carrying single-copy transgene insertions were generated by the Universal MosSCI system, according to previously published protocols (Frøkjær-Jensen et al., 2008). Transgenes with the pCFJ350 backbone were injected into EG6699 or EG8081 and the progeny were selected using selection markers. Insertions were verified by PCR. Multiple independent insertion lines were screened for expression of the transgenes.

The *pcmd-1(syb1285 syb486[gfp::pcmd-1(ΔCC)])I* allele was generated by SunyBiotech by deleting 33 amino acids from E86 including F118, spanning the coiled-coil domain ranging from amino acids E86 to N117, predicted by the COILS program (see below). The deletion was verified by PCR amplification using the oligos GCGCTCCGTTGAGAATCTCGTA and CACAAACGAGCCCGCACGGA and sequencing.

Protein domain prediction and illustration
IDRs were annotated based on information provided by the UniProt Consortium (UniProt Consortium, 2019). The coiled-coil domain was defined via the COILS program with a 28-residue window comparing both MTK and MTIDK matrices (weighted and unweighted) (Lupas et al., 1991; Lupas, 1996). The domain structures were illustrated using DOG2.0 (Ren et al., 2009).

Yeast strains, media and transformation

Growth and genetic manipulation of the *Saccharomyces cerevisiae* strain EGY 48/194 (MATα, trp 1, his 3, ura 3, leu2::2/4 LECAop-LEU2) were performed using standard genetic techniques. The yeast strain was transformed with plasmids using lithium acetate (1 M). The selection of the different plasmids was conducted with complete minimal medium lacking histidine/uracil/tryptophane/leucine. Yeast two-hybrid assays were performed using the Grow'N'Glow GFP Yeast Two-Hybrid System (Mobitech) according to the manufacturer's protocol. Full-length cDNA of *C. elegans* SAS-7, PCMD-1, PCMD-1(ΔCC), PCMD-1(C2), SPD-5, PLK-1 and SAS-4 were inserted into the bait vector pEG202 containing the DNA-binding domain LexA. pEG202_SPD-5 could not be used owing to autoactivation. The cDNA of the different candidates PCMD-1, PCMD-1(ΔCC), PCMD-1(C2), SPD-2, SPD-5, PLK-1, SAS-7 and SAS-4 were cloned into the prey vector pJG45 comprising the B42 transcription activation domain. The third plasmid transformed into the yeast was pGNG1-GFP containing the reporter gene *gfp*. pEG202-p53 with pJG45-LTA was used as a positive control, whereas pJG45 without an insert was used as a negative control. The presence of the plasmids in yeast was verified by plasmid extraction, followed by PCR amplification of the inserts and sequencing. Expression of the prey proteins was verified by immunoblotting against an HA-tag.

Cell lines and culture conditions

Human embryonic kidney (HEK) 293T cells were cultured at 37°C (5% CO_2) in Dulbecco's modified Eagle's medium (DMEM) supplemented with 10% fetal bovine serum (FBS; Biochrom), 100 units/ml penicillin and 100 µg/ml streptomycin (Gibco).

Co-immunoprecipitation

HEK293T cells were transfected with 4 µg DNA of pTMD143 and/or pTMD144. After 24 h, cells were chilled to 4°C. To prepare cell extracts, cells were washed once with 1×PBS and pelleted by centrifugation at 1000 ***g*** for 5 min. Cell pellets were lysed using 100 µl lysis buffer [10 mM Tris-HCl (pH8.0), 50 mM NaF, 0.3 mM Na_3VO_4, 10 mM sodium pyrophosphate, 5 mM β-glycerolphosphate, 120 mM NaCl, 0.25% NP40] containing protease and phosphatase inhibitors (PhosSTOP, Pefabloc, cOmplete Mini, Pepstatin A, Leupeptin, Sigma-Aldrich; Aprotinin, Carl Roth) by incubating them for 30 min at 4°C. Crude extracts were clarified by centrifugation at 12,000 ***g*** for 12 min at 4°C and incubated with RFP-trap agarose beads (ChromoTek). Beads were pre-blocked in 3% bovine serum albumin and washed three times in 500 µl lysis buffer before use. Beads were then collected by centrifugation at 2500 ***g*** for 5 min at 4°C, washed 1× in lysis buffer and resuspended in SDS gel loading buffer. The double volume was loaded for the CoIP compared with input (I) and flow-through (FT). Immunoblotting was performed by using primary antibodies mouse anti-GFP (1:1000; 11814460001, Sigma-Aldrich) and mouse anti-His (1:1000; MA1-135, Thermo Scientific) and HRP-linked anti-mouse secondary antibody [1:7500; Goat Anti-Mouse IgG (H+L)-HRP Conjugate, 170-6516, Bio-Rad)] and detected using ECL Prime Western Blotting Detection Reagent (Amersham).

Translocation assay

L4 stage worms of different strains carrying the construct with the heat-shock promoter (TMD151, TMD157, TMD158, TMD159, TMD162, TMD165, TMD168, TMD167, TMD183 and TMD184) were shifted to 25°C for 15 h. Subsequently, worms laid eggs for 2 h at 25°C. The embryos were mounted on a 2% agarose pad and heat-shocked at 30°C for 1 h (Thermocycler, Bio-Rad). After 2 h recovery at 20°C, embryos were imaged using a SP5 Leica confocal microscope (see 'Microscopy' section). Control embryos were incubated at 20°C without heat shock. Feeding RNAi against *spd-5* was performed for 20 h at 25°C by using I-2G08 for TMD168 and the pTMD118 feeding clone constructed against the re-encoded region (Woodruff et al., 2015, 2017; Mittasch et al., 2020) for TMD151 and TMD162. Soaking RNAi against *sas-4* for TMD183 and TMD184 was performed against the re-encoded region (Cottee et al., 2013). dsRNA was made using the MEGAscript T7 Kit (Invitrogen) and primers

TAATACGACTCACTATAGATGGCTTCCGATGAAAATATCGGTGC and TAATACGACTCACTATAGGCAGCGTGCTGTCCACTGTGGC. Worms were incubated in 1 µg/µl dsRNA for 48 h at 20°C and allowed to recover for 24 h at 25°C. Both RNAi treatments were validated on N2 worms by lethality tests and differential interference contrast (DIC) imaging. Embryos with a minimum of two cells in the case of a weak GFP signal or one cell with the GFP signal surrounding the whole circumference of this cell were considered as positive.

Marked mating experiments

To mark the sperm centrioles in marked mating experiments *fog-2(q71)*, females were mated with TMD119 males at 20°C and the progeny imaged by 4D microscopy. For the converse experiment, TMD119 L4 worms were fed *fem-1(RNAi)* overnight. The hatched progeny were raised on *fem-1(RNAi)* to block sperm production. Feminized animals were mated with *fog-2(q71)* males at 20°C. Progeny of the crosses were either imaged by 4D microscopy or used for indirect immunofluorescence. Meiotic stages of embryos in fixed samples were staged by the condensation state of the female DNA and the presence of the polar bodies.

Indirect immunofluorescence

Indirect immunofluorescence was performed using a protocol by Delattre et al. (2004). Hermaphrodite worms were cut in M9 buffer, covered with a coverslip, and placed on ice blocks. After freeze-cracking, slides were fixed in methanol, followed by incubation with primary antibodies anti-SAS-4 (1:500; sc-98949, Santa Cruz Biotechnology), anti-SPD-5 (1:1000, a generous gift from B. Bowerman; Hamill et al., 2002) and anti-GFP (1:500; 11814460001, Roche) overnight at 4°C and with Alexa 488-conjugated (1:500; A32723, Invitrogen Molecular Probes) and Alexa 568-conjugated (1:500; A-11011, Invitrogen Molecular Probes) secondary antibodies and Hoechst 33258 (1:1000, Sigma-Aldrich) at room temperature for 1 h.

Microscopy

Embryos treated for the translocation assay and indirect immunofluorescence samples were imaged at a resolution of 1024×1024 pixels with an HCX PL APO Lambda Blue 63×1.4 oil objective and a step size of 0.7 µm on a SP5 Leica confocal microscope using LAS software. For live-cell imaging, young adult worms were either dissected in 6 µl M9 and mounted on 2% agar pads or dissected in Polybead Microspheres 20.00 µm (diluted 1:10 in M9). Live-cell imaging was performed on an inverted Nikon Eclipse Ti spinning disc confocal microscope using an Andor DU-888 X-11056 camera (1024×1024 pixels), a 100×1.45-NA Plan-Apochromat oil immersion objective and controlled by NIS Elements 4.51 software. *z*-stacks were taken every 30 s with a step size of 0.7 µm and with 2×2 binning. Embryos for marked mating experiments were imaged using a Zeiss Axio Imager.M2 equipped with epifluorescence and 'Time to Live' software from Caenotec. Twenty-five DIC *z*-stacks were taken throughout the volume of the embryo every 35 s, and fluorescence scans were taken at required time points.

For SIM of live *C. elegans* embryos, we used the ZEISS Elyra 7 system in the Lattice SIM mode equipped with a Plan Apochromat 63×/1.40 oil immersion objective. Images were acquired with two pco.edge sCMOS 4.2 cameras simultaneously, using the ZEISS DuoLink adapter. Acquired *z*-stacks with a voxel size of $63×63×110$ nm^3 and field of view size of 1024×1024 pixels were processed using the SIM processing algorithm of ZEN Black 3.0 software. SIM processed *z*-stacks have a voxel size of $31.5×31.5×110$ nm^3. Yeast colonies were acquired using a Leica Stereomicroscope M205 FA, controlled by the Leica Application Suite software (3.2.0.9652) and equipped with a 1×2.11 NA Plan Apo lens and a Leica DigitalDFC340x FX camera.

Fluorescence intensity measurements

GFP and RFP intensities were measured on raw images by analyzing *z*-stacks with ManualTrackMate in Fiji (Tinevez et al., 2017). The time point was either defined through the DNA condensation visualized by the mCherry::H2B marker (for EU3000, TMD107, TMD165, TMD166,

TMD175, TMD177, TMD181, TMD202, TMD210) or through corresponding DIC recordings (for TMD119, TMD123, PHX1285, TMD178, TMD179, TMD203, TMD214, TMD216, TMD217). When there was no clear GFP signal recognizable, the centrosomal position was determined by DIC. A fixed radius was applied to measure all fluorescent signals (GFP::PCMD-1: 0.762 µm for Fig. 1E and 0.788 µm for all other figures, GFP::SAS-7: 0.828 µm, RFP::SPD-5: 4.062 µm), background signal, and cytoplasmic background signal outside the embryo, in 3D. Intensities were calculated for each centrosome as: intensity=(C-B)−(CS-B). The total intensity of the background (B) was subtracted from the total intensity of the centrosome (C) and from the total intensity of the cytoplasmic signal (CS). The cytoplasmic signal without background was then subtracted from the centrosomal signal without background. For GFP::SAS-7, the sum of the centrosomal fluorescence intensities per embryo was used to calculate the mean centrosomal fluorescence intensities because of separation defects in some *pcmd-1(t3421)* embryos. For cytoplasmic GFP values, the background (B) was subtracted from the cytoplasmic signal (CS).

Statistical analysis was performed by using R Studio version 1.2.5003 (R Core Team, 2014). Shapiro–Wilk test was used to test for normality. Levene's test was performed to compare variances. Depending on the normality, variance, and number of groups in the data sets, different comparison tests were performed (see figure legends). Mean values with the standard error of mean were plotted in Prism v6.

Circularity measurements

Centrosomal circularities were evaluated in one-cell embryos ranging from NEB to metaphase that were immunostained with an antibody against SPD-5. The cell stage was defined by DNA condensation, visualized with Hoechst staining. Image analysis was performed in Fiji (Schindelin et al., 2012). Maximum *z*-projections were created and the PCM shapes were converted into black/white outlines using the 'Huang' threshold. Statistical analysis was performed by using R Studio version 1.2.5003 (R Core Team, 2014). Shapiro–Wilk test was used to test for normality. Levene's test was performed to compare variances. Mann–Whitney *U*-Test was used for the comparison of circularity values. Mean values with the standard error of mean were plotted with Prism v6.

Statistical analysis for survival

L4 worms were singled and maintained at the indicated temperature for 16-20 h; laid eggs and hatched adult worms were counted. Statistical analysis was performed in R Studio version 1.2.5003 (R Core Team, 2014). Shapiro–Wilk test was used to test for normality. Levene's test was used to test for homogeneity of variances. Depending on the normality, variance, and number of groups in the data sets, different comparison tests were performed (see figure legends).

Author contributions

Conceptualization: E. Zanin, T.M.-D.; Methodology: L.S., A.S., E. Zanin, T.M.-D.; Validation: L.S., A.S., E. Zuccoli, T.M.-D.; Formal analysis: L.S., A.S., E. Zuccoli, T.M.-D.; Investigation: L.S., A.S., E. Zuccoli, S.Ü., J.M., T.M.-D.; Resources: L.S., A.S., E. Zuccoli, S.Ü., J.M., T.M.-D.; Data curation: T.M.-D.; Writing - original draft: L.S., T.M.-D.; Writing - review & editing: L.S., A.S., E. Zuccoli, E. Zanin, T.M.-D.;

Visualization: L.S., A.S., E. Zuccoli, T.M.-D.; Supervision: L.S., T.M.-D.; Project administration: T.M.-D.; Funding acquisition: T.M.-D.

References

Boxem, M., Maliga, Z., Klitgord, N., Li, N., Lemmens, I., Mana, M., de Lichtervelde, L., Mul, J. D., van de Peut, D., Devos, M. et al. (2008). A protein domain-based interactome network for *C. elegans* early embryogenesis. *Cell* **134**, 534-545. doi:10.1016/j.cell.2008.07.009

Brenner, S. (1974). The genetics of *Caenorhabditis elegans*. *Genetics* **77**, 71-94. doi:10.1093/genetics/77.1.71

Buchman, J. J., Tseng, H.-C., Zhou, Y., Frank, C. L., Xie, Z. and Tsai, L.-H. (2010). Cdk5rap2 interacts with pericentrin to maintain the neural progenitor pool in the developing neocortex. *Neuron* **66**, 386-402. doi:10.1016/j.neuron.2010.03.036

Cabral, G., Laos, T., Dumont, J. and Dammermann, A. (2019). Differential requirements for centrioles in mitotic centrosome growth and maintenance. *Dev. Cell* **50**, 355-366.e6. doi:10.1016/j.devcel.2019.06.004

Cottee, M. A., Muschalik, N., Wong, Y. L., Johnson, C. M., Johnson, S., Andreeva, A., Oegema, K., Lea, S. M., Raff, J. W. and van Breugel, M. (2013). Crystal structures of the CPAP/STIL complex reveal its role in centriole assembly and human microcephaly. *eLife* **2**, 23-30. doi:10.7554/eLife.01071

Dammermann, A., Müller-Reichert, T., Pelletier, L., Habermann, B., Desai, A. and Oegema, K. (2004). Centriole assembly requires both centriolar and pericentriolar material proteins. *Dev. Cell* **7**, 815-829. doi:10.1016/j.devcel.2004.10.015

Dammermann, A., Maddox, P. S., Desai, A. and Oegema, K. (2008). SAS-4 is recruited to a dynamic structure in newly forming centrioles that is stabilized by the gamma-tubulin-mediated addition of centriolar microtubules. *J. Cell Biol.* **180**, 771-785. doi:10.1083/jcb.200709102

Decker, M., Jaensch, S., Pozniakovsky, A., Zinke, A., O'Connell, K. F., Zachariae, W., Myers, E. and Hyman, A. A. (2011). Limiting amounts of centrosome material set centrosome size in *C. elegans* embryos. *Curr. Biol.* **21**, 1259-1267. doi:10.1016/j.cub.2011.06.002

Delattre, M., Leidel, S., Wani, K., Baumer, K., Bamat, J., Schnabel, H., Feichtinger, R., Schnabel, R. and Gönczy, P. (2004). Centriolar SAS-5 is required for centrosome duplication in *C. elegans*. *Nat. Cell Biol.* **6**, 656-664. doi:10.1038/ncb1146

Delattre, M., Canard, C. and Gönczy, P. (2006). Sequential protein recruitment in *C. elegans* centriole formation. *Curr. Biol.* **16**, 1844-1849. doi:10.1016/j.cub.2006.07.059

Erpf, A. C., Stenzel, L., Memar, N., Antoniolli, M., Osepashvili, M., Schnabel, R., Conradt, B. and Mikeladze-Dvali, T. (2019). PCMD-1 organizes centrosome matrix assembly in *C. elegans*. *Curr. Biol.* **29**, 1324-1336.e6. doi:10.1016/j.cub.2019.03.029

Fields, S. and Song, O.-K. (1989). A novel genetic system to detect protein-protein interactions. *Nature* **340**, 245-246. doi:10.1038/340245a0

Frøkjær-Jensen, C., Davis, M. W., Hopkins, C. E., Newman, B. J., Thummel, J. M., Olesen, S.-P., Grunnet, M. and Jorgensen, E. M. (2008). Single-copy insertion of transgenes in *Caenorhabditis elegans*. *Nat. Genet.* **40**, 1375-1383. doi:10.1038/ng.248

Galletta, B. J., Fagerstrom, C. J., Schoborg, T. A., McLamarrah, T. A., Ryniawec, J. M., Buster, D. W., Slep, K. C., Rogers, G. C. and Rusan, N. M. (2016). A centrosome interactome provides insight into organelle assembly and reveals a non-duplication role for Plk4. *Nat. Commun.* **7**, 12476. doi:10.1038/ncomms12476

Garbrecht, J., Laos, T., Holzer, E., Dillinger, M. and Dammermann, A. (2021). An acentriolar centrosome at the *C. elegans* ciliary base. *Curr. Biol.* **31**, 12476. doi:10.1016/j.cub.2021.03.023

Hamill, D. R., Severson, A. F., Carter, J. C. and Bowerman, B. (2002). Centrosome maturation and mitotic spindle assembly in *C. elegans* require SPD-5, a protein with multiple coiled-coil domains. *Dev. Cell* **3**, 673-684. doi:10.1016/S1534-5807(02)00327-1

Hilbert, M., Erat, M. C., Hachet, V., Guichard, P., Blank, I. D., Flückiger, I., Slater, L., Lowe, E. D., Hatzopoulos, G. N., Steinmetz, M. O. et al. (2013). *Caenorhabditis elegans* centriolar protein SAS-6 forms a spiral that is consistent with imparting a ninefold symmetry. *Proc. Natl. Acad. Sci. USA* **110**, 11373-11378. doi:10.1073/pnas.1302721110

Kemp, C. A., Kopish, K. R., Zipperlen, P., Ahringer, J. and O'Connell, K. F. (2004). Centrosome maturation and duplication in *C. elegans* require the coiled-coil protein SPD-2. *Dev. Cell* **6**, 511-523. doi:10.1016/S1534-5807(04)00066-8

DEVELOPMENT

Kirkham, M., Müller-Reichert, T., Oegema, K., Grill, S. and Hyman, A. A. (2003). SAS-4 is a *C. elegans* centriolar protein that controls centrosome size. *Cell* **112**, 575-587. doi:10.1016/S0092-8674(03)00117-X

Kitagawa, D., Vakonakis, I., Olieric, N., Hilbert, M., Keller, D., Olieric, V., Bortfeld, M., Erat, M. C., Flückiger, I., Gönczy, P. et al. (2011). Structural basis of the 9-fold symmetry of centrioles. *Cell* **144**, 364-375. doi:10.1016/j.cell.2011.01.008

Leidel, S. and Gönczy, P. (2003). SAS-4 is essential for centrosome duplication in *C. elegans* and is recruited to daughter centrioles once per cell cycle. *Dev. Cell* **4**, 431-439. doi:10.1016/S1534-5807(03)00062-5

Leidel, S., Delattre, M., Cerutti, L., Baumer, K. and Gönczy, P. (2005). SAS-6 defines a protein family required for centrosome duplication in *C. elegans* and in human cells. *Nat. Cell Biol.* **7**, 115-125. doi:10.1038/ncb1220

Lerit, D. A., Jordan, H. A., Poulton, J. S., Fagerstrom, C. J., Galletta, B. J., Peifer, M. and Rusan, N. M. (2015). Interphase centrosome organization by the PLP-Cnn scaffold is required for centrosome function. *J. Cell Biol.* **210**, 79-97. doi:10.1083/jcb.201503117

Lettman, M. M., Wong, Y. L., Viscardi, V., Niessen, S., Chen, S.-H., Shiau, A. K., Zhou, H., Desai, A. and Oegema, K. (2013). Direct binding of SAS-6 to ZYG-1 recruits SAS-6 to the mother centriole for Cartwheel Assembly. *Dev. Cell* **25**, 284-298. doi:10.1016/j.devcel.2013.03.011

Letunic, I. and Bork, P. (2018). 20 years of the SMART protein domain annotation resource. *Nucleic Acids Res.* **46**, D493-D496. doi:10.1093/nar/gkx922

Li, S., Armstrong, C. M., Bertin, N., Ge, H., Milstein, S., Boxem, M., Vidalain, P.-O., Han, J.-D. J., Chesneau, A., Hao, T. et al. (2004). A map of the interactome network of the metazoan *C. elegans*. *Science* **303**:540-543. doi:10.1126/science.1091403

Lupas, A., Van Dyke, M. and Stock, J. (1991). Predicting coiled coils from protein sequences. *Science* **252**, 1162-1164. doi:10.1126/science.252.5009.1162

Lupas, A. (1996). Prediction and analysis of coiled-coil structures. *Meth. Enzymol.* **266**, 513-525. doi:10.1016/s0076-6879(96)66032-7

Magescas, J., Eskinazi, S., Tran, M. V. and Feldman, J. L. (2021). Centriole-less pericentriolar material serves as a microtubule organizing center at the base of *C. elegans* sensory cilia. *Curr. Biol.* **31**, 2410-2417.e6. doi:10.1016/j.cub.2021.03.022

McNally, K. L. P., Fabritius, A. S., Ellefson, M. L., Flynn, J. R., Milan, J. A. and McNally, F. J. (2012). Kinesin-1 prevents capture of the oocyte meiotic spindle by the sperm aster. *Dev. Cell* **22**, 788-798. doi:10.1016/j.devcel.2012.01.010

Mittasch, M., Tran, V. M., Rios, M. U., Fritsch, A. W., Enos, S. J., Ferreira Gomes, B., Bond, A., Kreysing, M. and Woodruff, J. B. (2020). Regulated changes in material properties underlie centrosome disassembly during mitotic exit. *J. Cell Biol.* **219**, 623-647. doi:10.1083/jcb.201912036

O'Connell, K. F., Caron, C., Kopish, K. R., Hurd, D. D., Kemphues, K. J., Li, Y. and White, J. G. (2001). The *C. elegans zyg*-1 gene encodes a regulator of centrosome duplication with distinct maternal and paternal roles in the embryo. *Cell* **105**, 547-558. doi:10.1016/S0092-8674(01)00338-5

Pelletier, L., Özlü, N., Hannak, E., Cowan, C., Habermann, B., Ruer, M., Müller-Reichert, T. and Hyman, A. A. (2004). The *Caenorhabditis elegans* centrosomal protein SPD-2 is required for both pericentriolar material recruitment and centriole duplication. *Curr. Biol.* **14**, 863-873. doi:10.1016/j.cub.2004.04.012

Pelletier, L., O'Toole, E., Schwager, A., Hyman, A. A. and Müller-Reichert, T. (2006). Centriole assembly in *Caenorhabditis elegans*. *Nature* **444**, 619-623. doi:10.1038/nature05318

Qiao, R., Cabral, G., Lettman, M. M., Dammermann, A. and Dong, G. (2012). SAS-6 coiled-coil structure and interaction with SAS-5 suggest a regulatory mechanism in *C. elegans* centriole assembly. *EMBO J.* **31**, 4334-4347. doi:10.1038/emboj.2012.280

R Core Team. (2014). *R: A Language and Environment for Statistical Computing*. Vienna, Austria: R Foundation for Statistical Computing. URL http://www.R-project.org/.

Ren, J., Wen, L., Gao, X., Jin, C., Xue, Y. and Yao, X. (2009). DOG 1.0: illustrator of protein domain structures. *Cell Res.* **19**, 271-273. doi:10.1038/cr.2009.6

Rogala, K. B., Dynes, N. J., Hatzopoulos, G. N., Yan, J., Pong, S. K., Robinson, C. V., Deane, C. M., Gönczy, P. and Vakonakis, I. (2015). The *Caenorhabditis elegans* protein SAS-5 forms large oligomeric assemblies critical for centriole formation. *eLife* **4**, e07410. doi:10.7554/eLife.07410

Schindelin, J., Arganda-Carreras, I., Frise, E., Kaynig, V., Longair, M., Pietzsch, T., Preibisch, S., Rueden, C., Saalfeld, S., Schmid, B. et al. (2012). Fiji: an open-source platform for biological-image analysis. *Nat. Meth.* **9**, 676-682. doi:10.1038/nmeth.2019

Schultz, J., Copley, R. R., Doerks, T., Ponting, C. P. and Bork, P. (2000). SMART: a web-based tool for the study of genetically mobile domains. *Nucleic Acids Res.* **28**, 231-234. doi:10.1093/nar/28.1.231

Sugioka, K., Hamill, D. R., Lowry, J. B., McNeely, M. E., Enrick, M., Richter, A. C., Kiebler, L. E., Priess, J. R. and Bowerman, B. (2017). Centriolar SAS-7 acts upstream of SPD-2 to regulate centriole assembly and pericentriolar material formation. *eLife* **6**, e20353. doi:10.7554/eLife.20353

Tinevez, J.-Y., Perry, N., Schindelin, J., Hoopes, G. M., Reynolds, G. D., Laplantine, E., Bednarek, S. Y., Shorte, S. L. and Eliceiri, K. W. (2017). TrackMate: An open and extensible platform for single-particle tracking. *Methods* **115**, 80-90. doi:10.1016/j.ymeth.2016.09.016

UniProt Consortium. (2019). UniProt: a worldwide hub of protein knowledge. *Nucleic Acids Res.* **47**, D506-D515. doi:10.1093/nar/gky1049

Uversky, V. N. (2019). Intrinsically disordered proteins and their "Mysterious" (Meta)physics. *Front. Phys.* **7**, 1-18. doi:10.3389/fphy.2019.00010

Varadarajan, R. and Rusan, N. M. (2018). Bridging centrioles and PCM in proper space and time. *Essays Biochem.* **62**, 793-801. doi:10.1042/EBC20180036

Woodruff, J. B., Wueseke, O., Viscardi, V., Mahamid, J., Ochoa, S. D., Bunkenborg, J., Widlund, P. O., Pozniakovsky, A., Zanin, E., Bahmanyar, S. et al. (2015). Regulated assembly of a supramolecular centrosome scaffold in vitro. *Science* **348**, 808-812. doi:10.1126/science.aaa3923

Woodruff, J. B., Gomes, B. F., Widlund, P. O., Mahamid, J., Honigmann, A. and Hyman, A. A. (2017). The centrosome is a selective condensate that nucleates microtubules by concentrating tubulin. *Cell* **169**, 1066-1071.e10. doi:10.1016/j.cell.2017.05.028
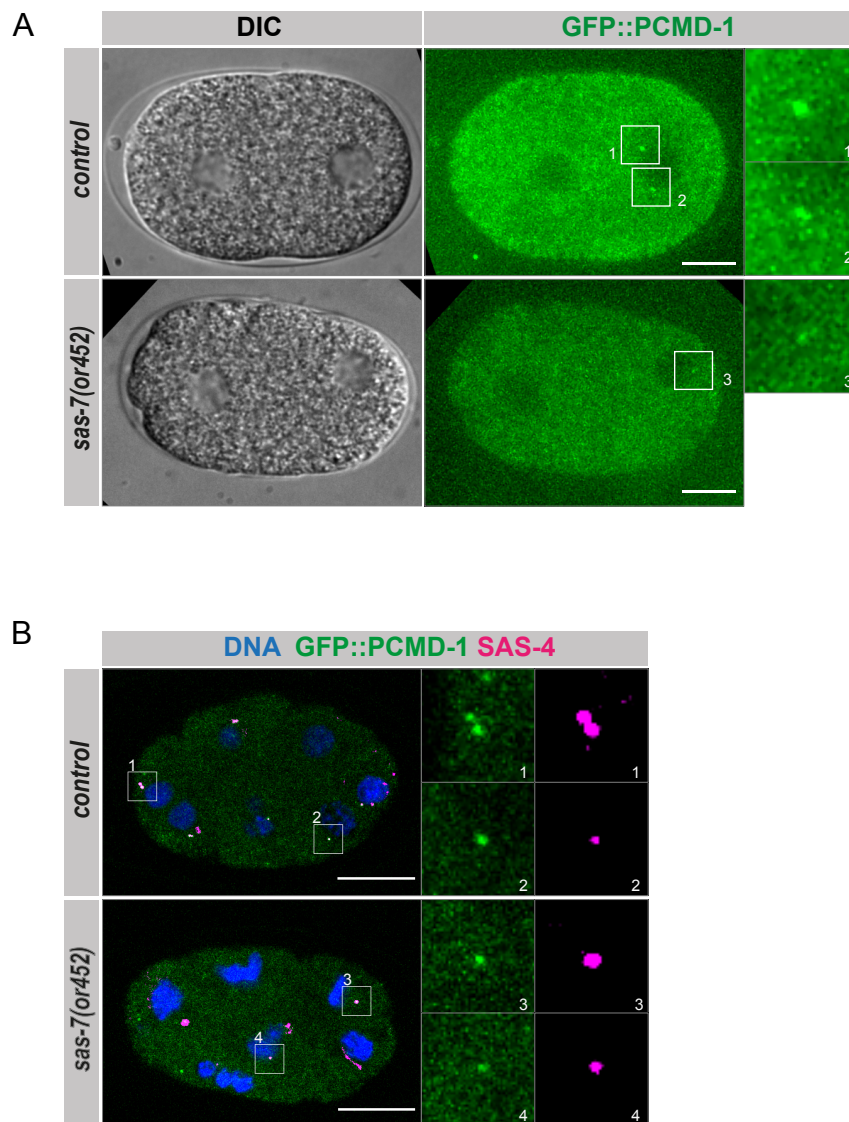
Fig. S1. SAS-7 recruits PCMD-1 to the centrioles in early embryos
(A) Stills of time-lapse spinning disc confocal images of *gfp::pcmd-1* (n=6) and *gfp::pcmd-1;sas-7(or452)* (n=8) embryos during pronuclear migration. Centrosomes are shown enlarged for the GFP::PCMD-1 signal.
(B) Representative confocal images of fixed *gfp::pcmd-1* (n=3) and *gfp::pcmd-1;sas-7(or452)* (n=8) embryos (>6 nuclei) stained for DNA, GFP and SAS-4. Insets represent single channels of the centrioles.
In all panels, scale bars are 10 μm.
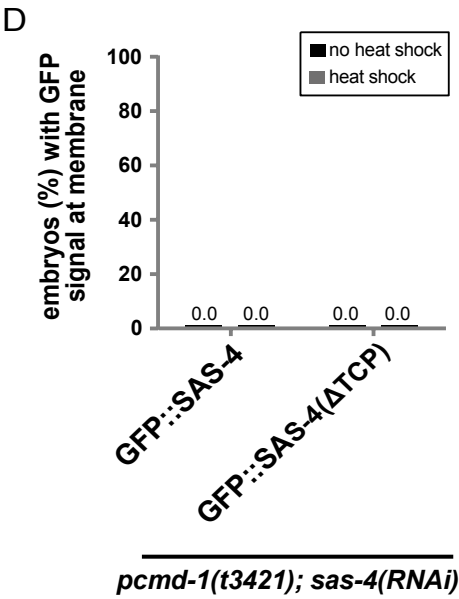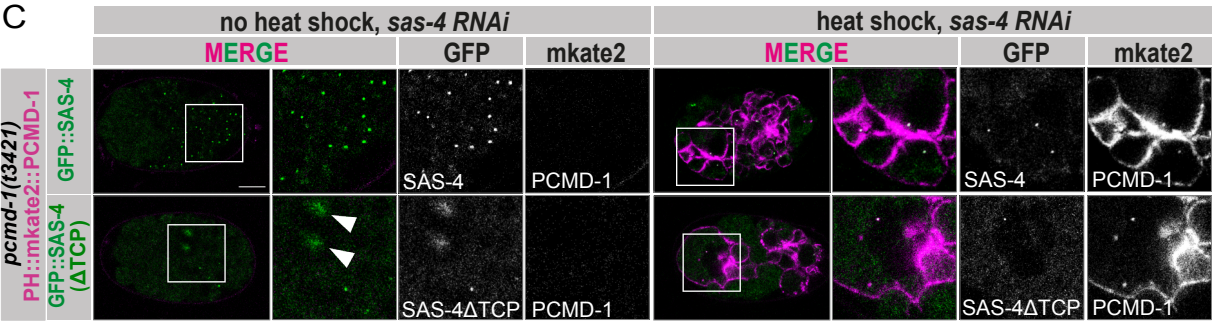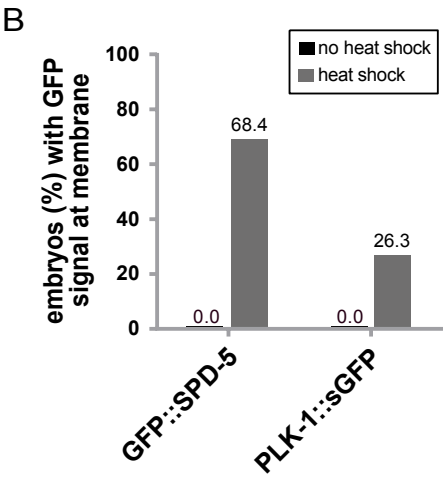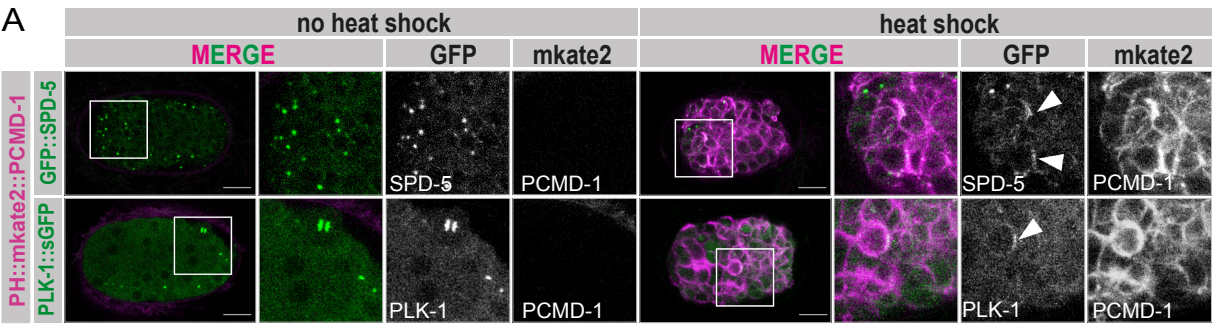
Fig. S2. PCMD-1 targeting of SPD-5 and PLK-1 to the plasma membrane in the presence of endogenous PCMD-1 is less efficient

(A) Representative multicellular embryos of the 'translocations assay' using GFP::SPD-5 (n=19 no heat shock; n=19 heat shock), and PLK-1::sGFP (n=20 no heat shock; n=19 heat shock) in a wild-type background. Selected regions are enlarged and shown as merge and single channels. Note that plasma membrane-localized PLK-1::sGFP is faint. Scale bars are 10 μm.

(B) Quantification of (A); the percentage of embryos (%) with GFP signal at the membrane after heat shock in the wild-type background.

(C) Representative multicellular embryos of the 'translocations assay' using GFP::SAS-4 (n=33 no heat shock; n=36 heat shock), and GFP::SAS-4(deltaTCP) (n=30 no heat shock; n=29 heat shock) in a *pcmd-1(t3421)* background and treated with *sas-4(RNAi)*. Selected regions are enlarged and shown as merge and single channels. Scale bars are 10 μm.

(D) Quantification of (C); the percentage of embryos (%) with GFP signal at the membrane after heat shock in the *sas-4(RNAi)* background.
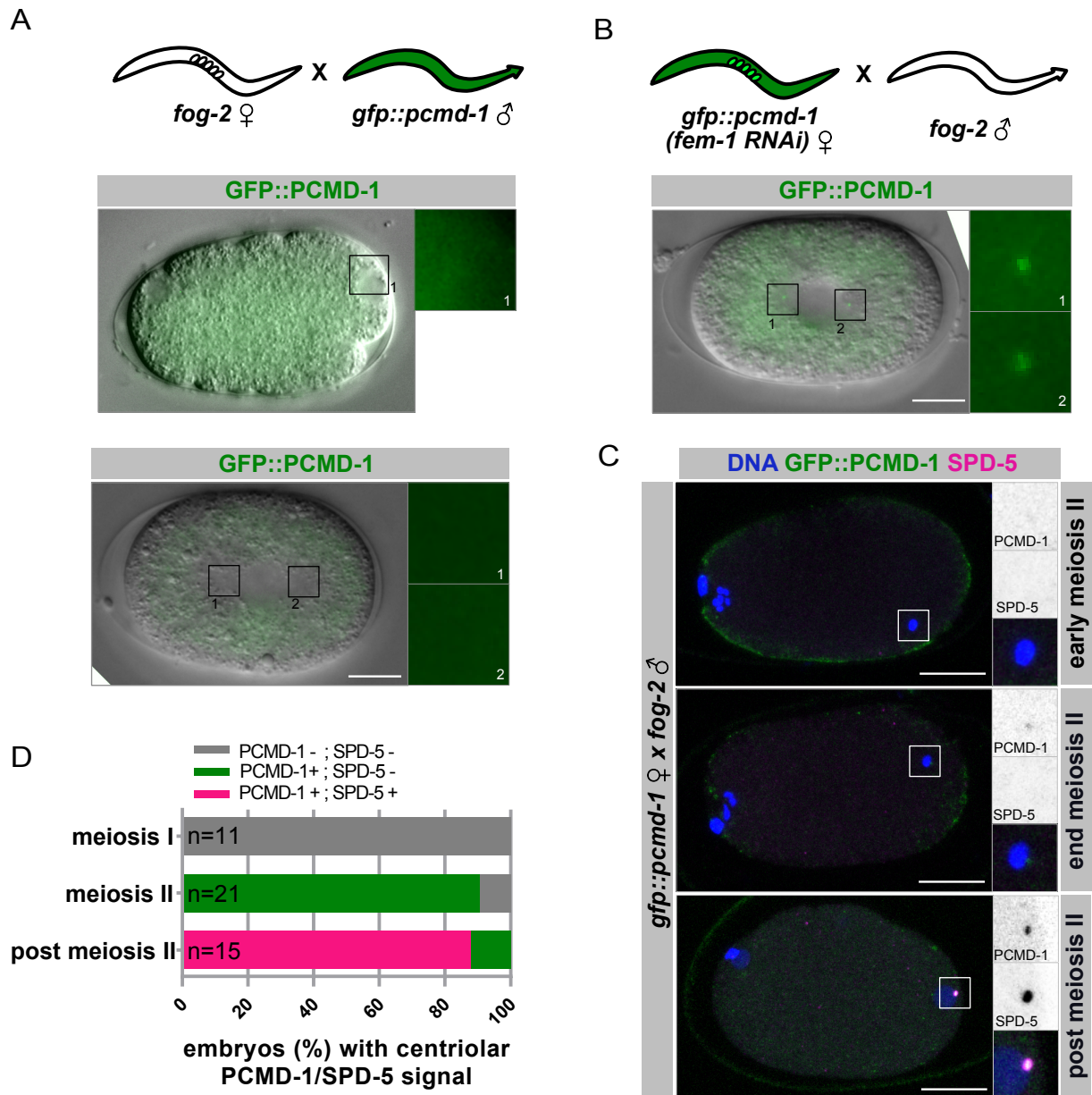
Fig. S3. PCMD-1 is recruited before SPD-5 to sperm-derived centrioles

(A) Schematic representation of a marked mating experiment where *fog-2(n71)* females were mated with *gfp::pcmd-1* males. The images below represent one-cell embryos taken by live-cell imaging shortly after meiosis II (n=6) and at metaphase (n=11). Centrosomal areas were determined by DIC imaging and are shown enlarged for the GFP::PCMD-1 signal.

(B) Schematic representation of a marked mating experiment where *fem-1(RNAi)*-treated *gfp::pcmd-1* females were mated with *fog-2(n71)* males (n=10). The image below represents a one-cell embryo taken by live-cell imaging. Centrosomal areas were determined by DIC imaging and are shown enlarged for the GFP::PCMD-1 signal.

(C) Images of fixed embryos in different stages of meiosis II, derived from the cross indicated in (B) and stained for DNA, GFP and SPD-5. Enlarged are sperm-associated centrosomal signals merged and as single channels.

(D) Quantification of (C) percentage of embryos (%).

Scale bars in all panels are 10 µm.
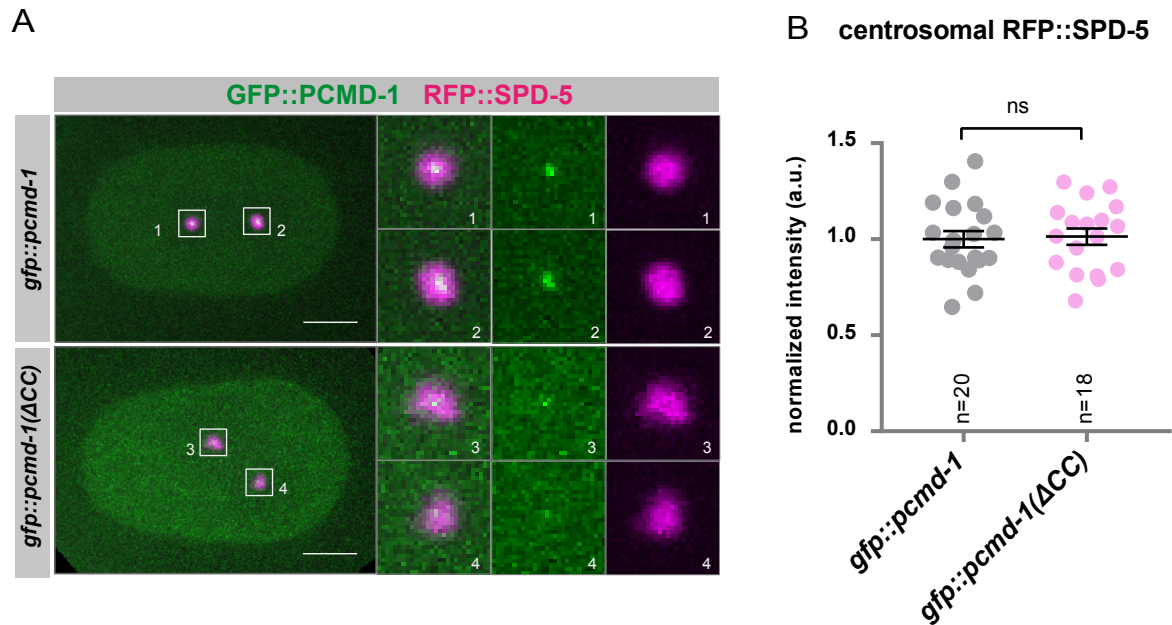
**Fig. S4. Deletion of the coiled-coil domain PCMD-1 does not affect centrosomal SPD-5 levels**
(A) Stills of time-lapse imaging of embryos expressing *rfp::spd-5 gfp::pcmd-1* (n=10) and
rfp::spd-5 gfp::pcmd-1(deltaCC) (n=9) at metaphase. Centrosomal areas are shown enlarged
as merge and for the RFP::SPD-5, GFP::PCMD-1 signal. n=number of embryos.
(B) Normalized centrosomal RFP signal intensities in embryos expressing *rfp::spd-5
gfp::pcmd- 1* and *rfp::spd-5 gfp::pcmd-1(deltaCC)* at metaphase. Two Sample t-test.
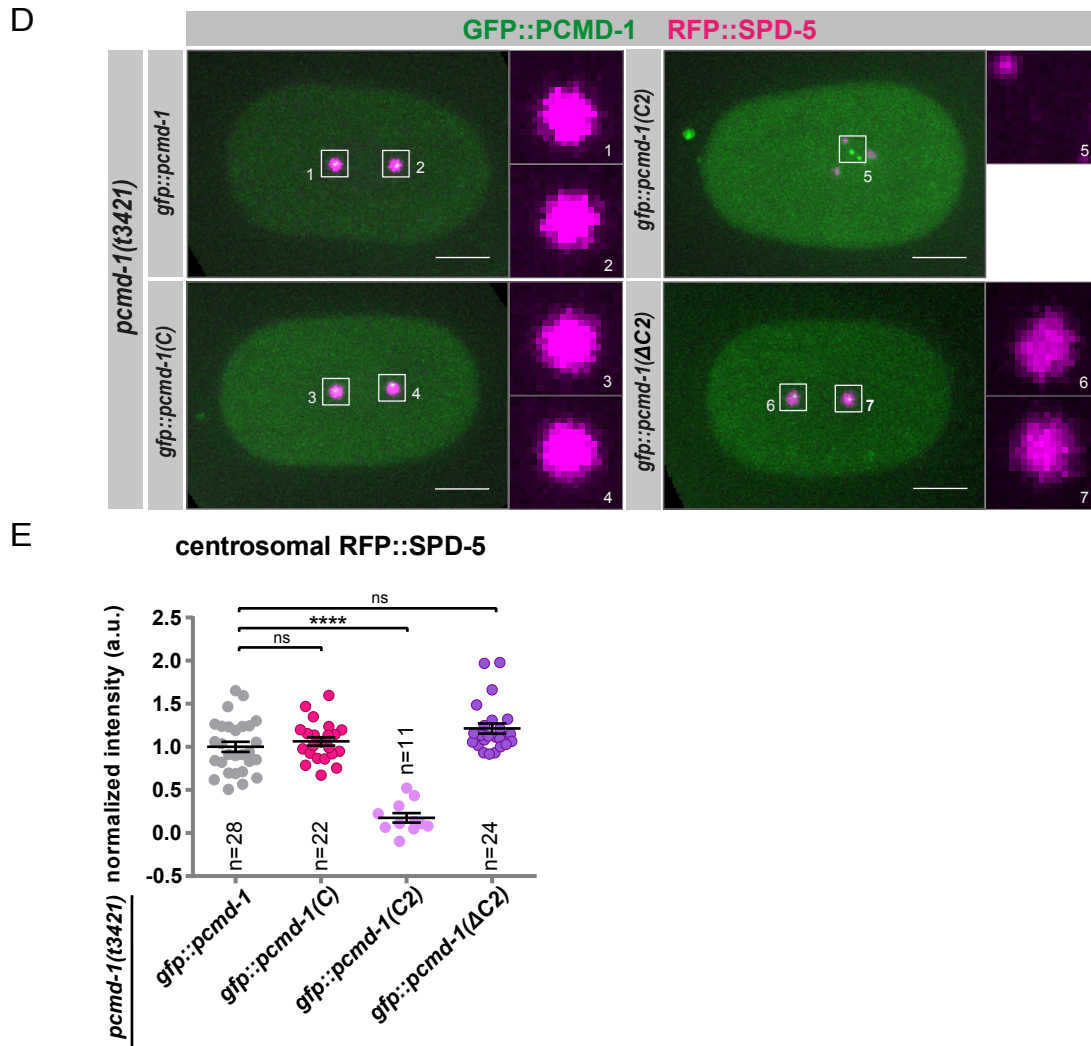n=number of analyzed centrosomes. ns $p > 0.05$. Scale bars are 10 µm.
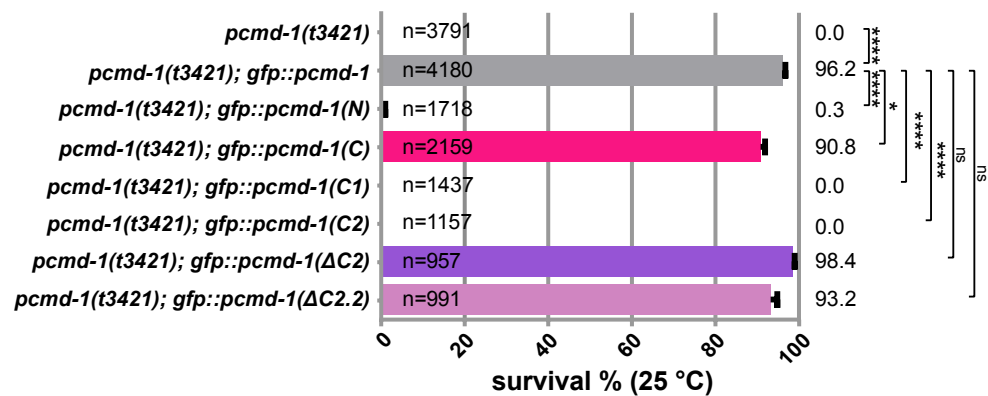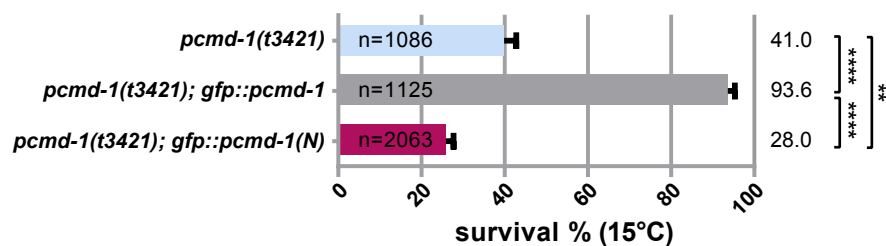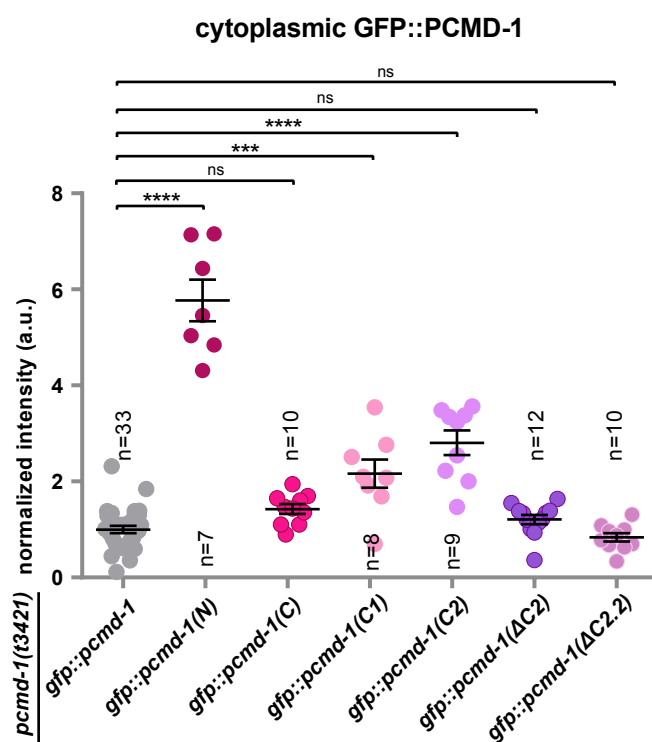
Fig. S5. The C2-region of PCMD-1 is insufficient to recruit SPD-5 to the centrosome

(A) Survival (%) of *gfp::pcmd-1, gfp::pcmd-1(N), gfp::pcmd-1(C), gfp::pcmd-1(C1), gfp::pcmd-1(C2), gfp::pcmd-1(deltaC2)* and *gfp::pcmd-1(deltaC2.2)* in the *pcmd-1(t3421)* background at 25C. Multiple Comparison with Kruskal Wallis test and post-hoc Dunn's test adjusted with Holm correction. n=number of analyzed embryos.

(B) Survival (%) of *gfp::pcmd-1* and *gfp::pcmd-1(N)* embryos in the *pcmd-1(t3421)* background at 15C. P-values were determined with multiple Comparison with Kruskal Wallis test and post-hoc Dunn's test adjusted with Holm correction, n=number of analyzed embryos.

(C) Normalized cytoplasmic GFP signal intensities of *gfp::pcmd-1, gfp::pcmd-1(N), gfp::pcmd-1(C), gfp::pcmd-1(C1), gfp::pcmd-1(C2), gfp::pcmd-1(deltaC2)* and *gfp::pcmd-1(deltaC2.2)* embryos, in combination with the *mCherry::h2b* in the *pcmd-1(t3421)* background at NEB. P-values were determined with multiple Comparison with Kruskal Wallis test and post-hoc Dunn's test adjusted with Holm correction, n=number of analyzed embryos.

(D) Stills of time-lapse imaging of *rfp::spd-5; gfp::pcmd-1* (n=14) and *rfp::spd-5; gfp::pcmd-1(C)* (n=11), *rfp::spd-5; gfp::pcmd-1(C2)* (n=9) and *rfp::spd-5; gfp::pcmd-1(deltaC2)* (n=12) of embryos in the *pcmd-1(t3421)* background at metaphase. Note that in two *rfp::spd-5; gfp::pcmd-1(C2) embryos* the PCM does not co-localize with the centrioles. Centrosomal areas are shown enlarged as merge and for the RFP::SPD-5, GFP::PCMD-1 signal. n=number of embryos.

(E) Normalized centrosomal RFP::SPD-5 signal intensities at metaphase of embryos in (D). p-values were determined with Multiple Comparison with Kruskal Wallis test and post-hoc Dunn's test adjusted with Holm correction, n=number of analyzed centrosomes.

In all panels error bars denote s.e.m. p-values represent: **p<0.01, ***p<0.001, ****p<0.0001, ns p>0.05. Scale bars are 10 µm.
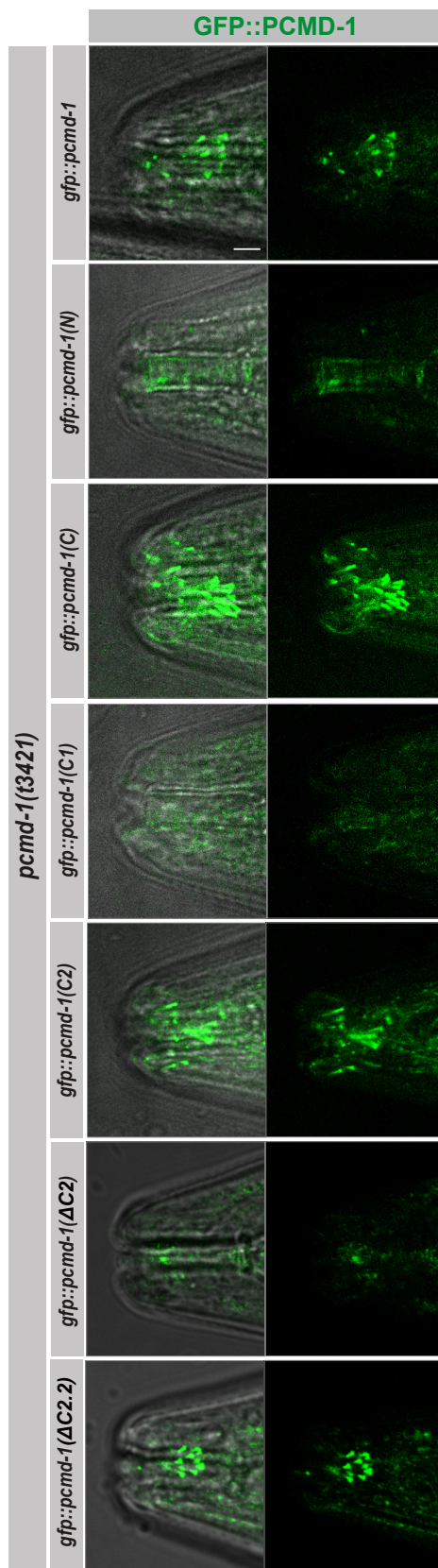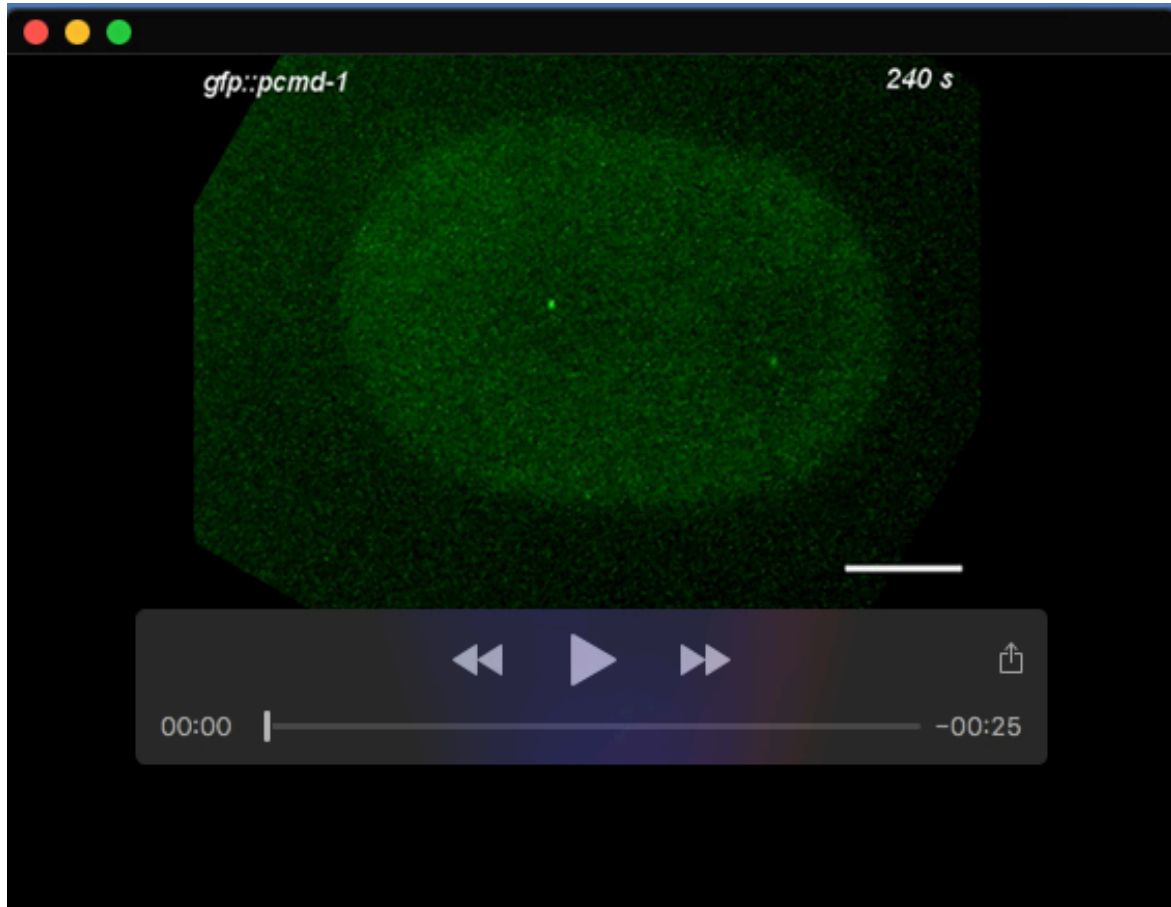
Fig. S6. The region spanning the IDR6 is necessary for ciliary targeting of PCMD-1
Localization of GFP::PCMD-1, GFP::PCMD-1(N), GFP::PCMD-1(C), GFP::PCMD-1(C1), GFP::PCMD-1(C2), GFP::PCMD-1(deltaC2) and GFP::PCMD-1(deltaC2.2) to the ciliary base in adult animals. n=5 animals for each condition.
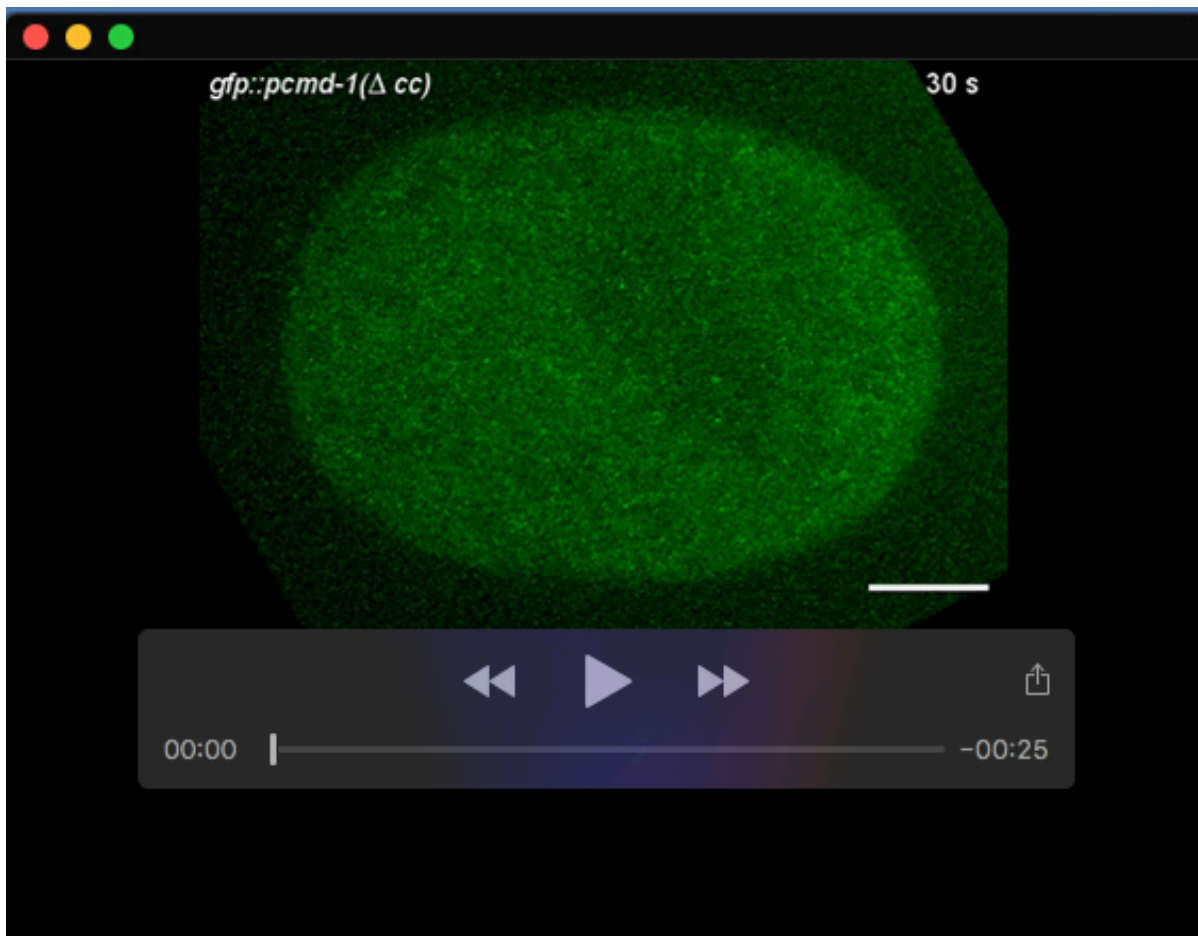Scale bars are 10 μm.

Table S1. Strains and materials used in the study.

Click here to download Table S1

Movie 1. Time-lapse of the first cell cycle of a GFP::PCMD-1 expressing embryo (related to figure 4C). In the control embryo, GFP::PCMD-1 localizes to the centrosome throughout the first cell cycle. Live-cell spinning disk microscopy. The scale bar is 10 μm.

Movie 2. Time-lapse of the first cell cycle of a GFP::PCMD-1 expressing embryo lacking the predicted coiled-coil domain (related to figure 4C) In the *gfp::pcmd-1(ΔCC)* embryo, GFP::PCMD-1(ΔCC) localizes to the centrosome with reduced levels. Live-cell spinning disk microscopy. The scale bar is 10 μm.